University of Alberta

A Novel Approach to DNA Transfection of E.coli DH5α Cells Using a Microfluidic Chip

By

Ehsan Majid

A thesis submitted to the faculty of Graduate studies and Research in Partial fulfillment of the requirements for the degree of Master of Science

Department of Chemistry

Edmonton, Alberta.

Spring 2003

National Library of Canada
Acquisitions and Bibliographic Services
395 Wellington Street
Ottawa ON K1A 0N4
Canada

Bibliothèque nationale du Canada
Acquisitions et services bibliographiques
395, rue Wellington
Ottawa ON K1A 0N4
Canada

Your file Votre référence

Our file Notre référence

The author has granted a non-exclusive licence allowing the National Library of Canada to reproduce, loan, distribute or sell copies of this thesis in microform, paper or electronic formats.

L'auteur a accordé une licence non exclusive permettant à la Bibliothèque nationale du Canada de reproduire, prêter, distribuer ou vendre des copies de cette thèse sous la forme de microfiche/film, de reproduction sur papier ou sur format électronique.

The author retains ownership of the copyright in this thesis. Neither the thesis nor substantial extracts from it may be printed or otherwise reproduced without the author's permission.

L'auteur conserve la propriété du droit d'auteur qui protège cette thèse. Ni la thèse ni des extraits substantiels de celle-ci ne doivent être imprimés ou autrement reproduits sans son autorisation.

0-612-82306-7

Canada

University of Alberta

Library Release Form

Name of Author:	Ehsan Majid
Title of Thesis:	A Novel Approach to DNA Transfection of E.coli DH5α Cells using a Microfluidic Chip.
Degree:	Master of Science
Year this Degree Granted:	2002

Permission is hereby granted to the University of Alberta Library to reproduce single copies of this thesis and to lend or sell such copies for private, scholarly or scientific research purposes only.

The author reserves all other publication and other rights in association with the copyright in the thesis, and except as herein before provided, neither the thesis nor any substantial portion thereof may be printed or otherwise reproduced in any material form whatever without the author's prior written permission.

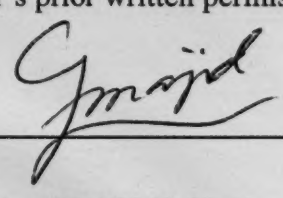

Apt #4, 10940 53 Ave
Edmonton, Alberta
Canada T6H 0S3

December 23, 2002

University of Alberta

Faculty of Graduate Studies and Research

The undersigned certify that they have read, and recommended to the Faculty of Graduate Studies and Research for acceptance, a thesis entitled **"A Novel Approach to DNA Transfection of E.coli DH5α Cells Using a Microfluidic Chip"** submitted by **Ehsan Majid** in partial fulfillment of the requirements for the Degree of **Master of Science**.

Supervisor: Dr. D. Jed Harrison

Dr. John-Bruce D. Green

External Examiner: Dr. Michael Deyholos

Dec 17, 2002

Date

Abstract

Microfluidic devices are recently being used for various microbiological purposes. The process of perforating living cells and transfecting them with different biological moieties, a process commonly known as electroporation was performed on chip by flowing E.coli DH5α cells through a single channel and applying high voltage pulses across a small segment. Cells were treated with fluo-4 dye before exposure to these pulses in presence of Ca^{2+}. Detection using a PMT was used to monitor the fluorescence due to the formation of Ca^{2+} and fluo-4 complex within the cells after electroporation. Similar experiments were performed using ampicillin resistant pbskII and GFP(uv) plasmid instead of Ca^{2+} and no dye. The cells were pumped out of the chip, diluted with LB broth and cultivated on ampicillin resistant agar plates in order to determine transfection efficiencies. Due to poor transfection efficiencies from insufficient electric field, leakage and clogging effects in the chip, a new device was designed, fabricated and tested. Transfection efficiencies obtained from this device differ from commercially available instruments by 1 to 2 orders of magnitude.

Acknowledgements

On completion of my master's thesis I would like to make a number of acknowledgements to individuals whose earnest encouragement and constant assistance have helped me accomplish yet another goal towards my professional career.

I feel a deep sense of gratitude towards my supervisor, Dr. Jed Harrison. I shall cherish all that he has given me in these few years as a mentor, guide and friend. I would like to thank him for guidance, constructive advice, financing various workshop and conference trips home and abroad, and above all, for his patience with me.

Among all the Harrison group members who have made my stay here at the department a wonderful experience, I would like to mention a few names in particular. Dr. Said Attiya and Dr. Fahima Ouchen for providing me technical assistance as a new graduate student; Abebaw Jemere, Justine Taylor, James Bao and Vasile Furdui for their fruitful suggestions and pleasant times in the lab. I would like to express my sincere appreciation to Arlene Figley who has helped me in numerous day to day chores in the department. Her kindhearted nature and willingness to help will inspire me to help others in the near future.

Special thanks to Dr. Monica Palcic for lots of good advice and unlimited access to her lab facilities. Thanks to my defense examiners Dr. John-Bruce Green and Dr. Michael Deyholos.

I am indebted to my wife Takrima, for all her support and care during the compilation of the manuscript. I do not know how to repay her for all the harsh times she went through. Finally I express my gratitude to the Almighty for giving me the strength and courage to sustain during the tenure of my research.

Table of Contents

Chapter 1: Introduction

1.1	**Miniaturaized Total Analysis System (μTAS): An Overview**	**1**
1.2	**Cell Transfection**	**2**
1.2.1	DEAE Dextran Method	3
1.2.2	Calcium Phosphate Method	3
1.2.3	Liposome Mediated Transfection	4
1.2.4	Retrovirus Mediated Gene Transfer	4
1.2.5	Biolistic Particle Delivery	4
1.2.6	Microinjection	5
1.2.7	Advanced Transfection Techniques	5
1.2.8	Electroporation	5
1.2.8.1	Mechanism of Electroporation	6
1.2.8.2	Electroporation of Bacterial Cells	7
1.2.8.3	Advantages of Bacteria Cell Electroporation	8
1.2.8.4	Figures of Merit for Bacteria Electroporation	9
1.2.8.5	Applications of Electroporation	9
1.3	**Electrokinetic μ-chip Devices – Recent Developments**	**11**
1.4	**Electro Osmotic and Pressure Driven Flow Systems**	**14**
1.4.1	Generation of EOF in Capillaries - The Double Layer Theory	14
1.4.2	Factors Influencing EOF	16
1.4.3	Pressure Driven Flow	16
1.5	**Cells on a Chip: An Overview**	**17**
1.6	**The Scope of this Thesis**	**19**
1.7	**References**	**21**

Chapter 2: DNA Transfection of E. coli Using a Microfluidic Chip

2.1	**Introduction**	**25**
2.2	**Experimental**	**27**
2.2.1	Device Fabrication and Instrumentation	27
2.2.2	Cell Growth and Preparation	28
2.2.3	Chip Operation	30
2.3	**Results and Discussion**	**31**
2.3.1	Device Design	31
2.3.1.1	Detailed Analysis of Geometric Effects on Electric Field and Flow	31
2.3.2	Operational Parameters and Chip Performance	38
2.3.3	Electroporation and Ca Ion Uptake	41
2.3.4	Electroporation and Transfection	42
2.4	**Conclusions**	**44**
2.5	**References**	**46**

Chapter 3: Single Channel Electroporator for Higher Transfection Efficiency

3.1	**Introduction**	**47**
3.2	**Design Concepts**	**50**
3.2.1	Embedded Electrode Design	50
3.2.2	Single Channel Electroporator	54
3.2.2.1	Evaluation of E, T_{por} and Transfection Efficiency	56
3.2.2.2	Determination of Resistance to Pressure Driven Flow	60
3.3	**Experimental**	**61**
3.3.1	Chip Design	61
3.3.2	Chip Fabrication: Problems, Solutions, and Real Time Chip Performance	63
3.3.2.1	Constant Channel Depth Upon Deep Etch	63
3.3.3	Transfection Parameters to be Optimized	63
3.3.4	Cell Growth, Preparation and Chip Operation	64
3.4	**Results and Discussion**	**66**
3.4.1	Designing Special Icons for a Double Mask Deep Etch Technique	66
3.4.2	Streak Marks of Photoresist on Substrate	68
3.4.3	DNA and Cell Concentration	68
3.4.4	Determination of Re-Circulating Flow in Channel	70
3.4.5	Dependence of Transfection Efficiency on Electric Field and Pulse Time	70
3.4.6	Effect of Cell and DNA Concentration on Transfection Efficiency	74
3.4.7	Chip Sensitive Parameters	77
3.4.7.1	Adding Salts to Media During Electroporation	77
3.4.7.2	Addition of Broth to Cell Receiving Reservoir and Duty cycle	78
3.5	**Conclusions**	**79**
3.6	**References**	**80**

Chapter 4: Conclusions and Future Developments

4.1	**Summary**	**81**
4.2	**Future Work**	**82**
4.2.1	Elimination of EOF in channels	82
4.2.2	Electroporation under Reduced Temperatures	83
4.2.3	Mammalian Cell Transfection	83
4.2.4	Integration to Other On-Chip Processes	83
4.2.5	Electroporation using Alternating Current (AC) Electric Fields	84
4.3	**References**	85

List of Tables

Table 1.1	Factors influencing EOF	**16**
Table 2.1	Dimensions for different sections of the hydro chip	**33**
Table 2.2	CFU and pulse time data for 3 μm weir hydrochip	**44**
Table 3.1	(a) parametres for transfection of common bacteria cell lines	**48**
	(b) Transfection parameters for common mammalian cell lines	**49**
Table 3.2	Electric field strengths between two metal plates separated by different gaps	**52**
Table 3.3	Maximum electric field strength to avoid bubbles for different frequencies applied to electrodes spaced 300 μm apart, at different NaCl concentrations	**53**
Table 3.4	Pulse times for a single channel electroporator with different weir lengths and voltages	**55**
Table 3.5	Values for pressure drops across channels for different dimension porator devices	**58**
Table 3.6	Weir lengths for porator chip	**62**
Table 3.7	Parameters for efficiency vs electric field studies	**72**
Table 3.8	Parameters for efficiency vs flow rate studies	**73**
Table 3.9	Parameters for Plasmid concentration studies	**75**
Table 3.10	Parameters for cell concentration studies	**76**

List of Figures

Figure 1.1	Induction of a transmembrane potential of a cell exposed to an electric field.	**7**
Figure 1.2	The diffuse double layer	**15**
Figure 1.3	(a) Laminar flow profile for pressure driven flow	**17**
	(b) Plug flow profile for EOF	**17**
Figure 2.1	(a) Sketch of chip showing labeling scheme	**27**
	(b) Equivalent electrical circuit	**27**
Figure 2.2	(a) Diagram of side arm showing weir and connecting channels	**32**
	(b) circuit diagram to determine resistance to flow	**32**
Figure 2.3	Graph of electric field and residence time as a function of applied voltage	**41**
Figure 2.4	Graph of fluorescence as a function of applied voltage	**42**
Figure 2.5	Graph of transfection efficiency as a function of electric field	**43**
Figure 2.6	Transfected colonies on agar plates	**44**
Figure 3.1	Graphs of minimum pulse time vs nominal flow rate	
	(1) pump flow and EOF in the same direction	**59**
	(2) opposite direction	**59**
Figure 3.2	(a) Single channel porator with tapered channels	**61**
	(b) without tapered Channels	**61**
Figure 3.3	Layout of poratorchip showing an array of 32 devices on a single 4" x 4" wafer	**62**
Figure 3.4	Device to connect peak tubing to microchip	**66**
Figure 3.5	(a) Icon for a shallow etch double mask process	**67**
	(b) Icon for a regular double mask process	**68**
Figure 3.6	Graph of Electric field versus efficiency	**72**
Figure 3.7	graph of efficiency vs pulse time	**73**
Figure 3.8	Graph of Efficiency vs plasmid concentration	**74**
Figure 3.9	Graph of Efficiency vs cell concentration	**76**

List of Abbreviations

Units

ms	Mili second (10^{-3})
μL	Micro liter (10^{-6})
μm	Micron (10^{-6})
μg	Micro gram (10^{-6})
ng	Nano gram (10^{-9})
CFU	Colony forming unit

Symbols

ζ	Zeta potential
κ	Debye layer thickness
ε	Permitivity of electrolyte
η	Viscosity
ρ	Resistivity
ϕ	Volumetric flow rate
$\Delta\Psi$	Potential difference between extra and intra cellular cell surface
μ_{eof}	Mobility due to electro osmotic flow
v_{eof}	Linear velocity due to electro osmotic flow
T_{por}	Pulse time/ Residence time
R	Resistance
K	Boltzman's constant
T	Absolute temperature
N	Avagadro's constant
I	Ionic strength
G_m	Membrane conductance per unit area
C_m	Membrane capacitance per unit area

Abbreviations

μTAS	Micro Total Analysis Systems
DEAE	Diethylaminoethyl
E.coli	*Escherichia coli*
PDMS	Poly(dimethylsiloxane)
PMMA	Polymethylmethacrylate
EOF	Electro osmotic flow
DMF	dimethylformamide
X-gal	5-bromo-4-chloro-3-indolyl-beta-D-galactopyranoside
IPTG	Isopropyl-beta-D-thiogalactopyranoside
GFP	Green fluorescent protein

Chapter 1: Introduction

1.1 Miniaturaized Total Analysis System (μTAS): An Overview

Since its inception in the early nineties by Micheal Widmer and co-workers [1] from the central research laboratories of Ciba Geigy in Beisel, Switzerland Micro-Total Analysis Systems (μTAS), has become a rapidly expanding and diversified research field of overwhelming popularity spanning the frontiers of the world of miniaturization. The need to automate an analytical process emerged from the realization that these systems resulted in less human error and lead to the concept of a "total analysis system" (TAS) [2]. In a TAS the basic components of an analytical process, i.e., sample processing, mixing chemical reactions, separations, and detection were all automated and integrated. Online glucose analyzers [3] and high speed capillary electrophoresis for separation are among the first examples of components incorporated in a TAS. The need to scale down dimensions and miniaturize such devices started a new era of micro-TAS, which became very popular upon the realization that these microsystems would yield faster analysis times and lower reagent consumption.

The pioneering work of S. C. Terry and co-workers [4] in 1979 on a gas chromatograph etched on a 5 cm silicon chip is one of the earliest demonstrations of miniaturization of a chemical instrument. The first condensed fluid devices that integrated separations were based upon capillary electrophoresis, combined with sample injection. These systems were miniaturized on planer glass chips by D. J. Harrison and A. Manz [5], representing a milestone that paved the way for the development of future, more complex, on-chip electrophoretic devices. They were the first to use photolithography and chemical etching techniques to etch capillaries on a glass surface to

perform electrophoretic separation. Since then there has been an ever increasing number of applications integrated on glass chips. The possibility of faster separations, and improved separation efficiency per unit time, along with lower sample consumption, and the fact that microsystems could be utilized for parallel processing to enhance higher throughput, initiated a drive towards the development of microdevices capable of handling multiple samples on a single device. Such a device described by Mathies et al. [6] consisted of a 10 cm diameter microchip capable of handling 96 DNA samples simultaneously, with a fragment sizing throughput as fast as one sample per second. Numerous applications of microfluidic devices in the field of analytical chemistry, genomics, proteomics, immunology, cellomics, etc, are now being demonstrated at an overwhelming rate.

The goal of this thesis was to develop a microfluidic device that would perform cell electroporation and gene transfection. Such a component could prove to be a more effective means of electroporation, and will extend the useful range of microchip techniques, providing more chip-based tools for genomics researchers. The introductory chapter deals with a review of recent microfluidic devices; electrokinetically driven ones in particular, followed by a relevant literature review of "cells on a chip." An introduction to electro-osmotic and pressure driven flow in glass chips will also be presented. Finally, an introduction to gene transfection and electroporation in particular will be discussed.

1.2 Cell Transfection

The method by which foreign bio molecules such as RNA, proteins, drugs, metabolites, etc, and DNA in particular are inserted into cells is known as transfection. It

is a powerful tool in the study and control of gene expression. Different techniques in cell transfection have been utilized to characterize different biochemical processes, cell growth behavior, effects of regulatory elements, etc. There are mainly two types of tranfection. The first is transient cell transfection, in which transfected DNA penetrates the nucleus of the cell, but does not integrate itself with the chromosomal DNA. In such transfection, many copies of the transfected gene are replicated, leading to high levels of expressed proteins. It is called transient because the expression of protein is short lived (24-72 hours). Stable transfection is the second type of transfection, in which DNA is integrated with the chromosomal DNA. There are a number of methods by which cell transfection is accomplished. These methods are discussed in the next few sections.

1.2.1 DEAE Dextran Method

Introduced in 1965 by A. Vaheri et al. [7] this method is one of the oldest methods of transfecting mammalian cells. Diethylaminoethyl (DEAE) dextran, which is a positively charged molecule, interacts with the negatively charged phosphate backbone of DNA to form a DNA-DEAE complex, which is adsorbed on the cell surface. The DNA is then taken up into the cytoplasm of the cell by a process called endocytosis. Relative simplicity and reproducibility are the main advantages of this method. Disadvantages include cytotoxic effects. This process is preferably used for transient cell transfection.

1.2.2 Calcium Phosphate Method

This method was first introduced in 1973 by F. L. Graham [8] to introduce adenovirus DNA into mammalian cells. DNA is mixed with phosphate buffer containing $CaCl_2$. The resulting calcium phosphate-DNA complex adheres to the cell surface and is

taken into the cytoplasm by endocytosis. This kind of transfection is suitable for stable transfection, however the reproducibility is low and many cell lines resist this kind of DNA transfer.

1.2.3 Liposome Mediated Transfection

First introduced by Felgher and co-workers [9] in 1987, this method involves complex formation between positively charged liposome and negatively charged phosphate backbone of DNA, followed by cell adsorption and endocytosis. It has higher reproducibility and efficiency than the DEAE dextran and calcium phosphate method. One drawback is the presence of serum during the transfection step lowers the yield. However, the absence of serum often increases the cytotoxicity of the liposome.

1.2.4 Retrovirus Mediated Gene Transfer

Cell transfection using retroviruses to transfer nonviral genes into miotic cells [10] is a method to perform stable transfection. This method is used to integrate a single copy of DNA into the host chromosome. It is a useful tool to incorporate genes into cells that are difficult to transfect. However, its use is biologically hazardous, and the method is much more complex than the dextran, calcium phosphate and liposome mediated gene transfection methods.

1.2.5 Biolistic Particle Delivery

In this method DNA is precipitated onto a microscopic gold particle. The particle is then shot into the cell using a ballastic device known as a gene gun. It is useful for human epithelial, fibroblast and lymphocyte transfection [11].

1.2.6 Microinjection

In this method, genes are directly injected into the nucleus within the embryo resulting in chromosomal integration [12] leading to recombinant genes. However, the method is restricted to a limited number of cell lines.

1.2.7 Advanced Transfection Techniques

A more efficient way of transfecting is with the help of activated dendrimer molecules. Dendrimer molecules are large spherical molecules with branches radiating from a central core atom [13]. The branches terminate with charged amino groups that can be used to interact with DNA molecules to form a dendrimer-DNA complex that adheres to the cell surface and is taken up within the cell by endocytocis [14]. Due to the efficient binding of DNA to the dendrimer, this method gives higher transfection efficiency.

1.2.8 Electroporation

Electroporation is a process by which living cells are exposed to an external high intensity electric field in order to create pores through which exogenous molecules may penetrate. It can be considered as a microinjection system used to incorporate specific components within the cellular media. In the 1950s and 60s several publications showed that an electric field applied to a cell induced a large transmembrane potential across two poles of a cell [15]. Later, in 1967, Sale and Hamilton [16] discovered that extremely high electric fields could cause cell lysis. By the early 70s it was established by several research groups that high electric fields at some critical value causes dielectric breakdown of the cell membrane. This was demonstrated with red blood cells by Crowley [17] and Zimmerman et al. [18]. Similar experiments with membranes were

performed by Newmann and Rosenheck [19]. By the late 70s Kinosita and Tsong [20] developed the concept of pore formation on the cell surface during dielectric breakdown of the cell wall. During the same period it was discovered that these cells could recover after application of the high intensity electric field, implying that electric field mediated pores were resealable and could be created without damaging the cell [21]. By the early 80s it was apparent that very small molecules can penetrate the electric field induced pores. Zimmerman et al. [22] first transfected cells with drugs in 1980. Catacholamine and calcium EDTA tranfection were first introduced in 1982 by Knight and Baker [23]. The first reports of DNA tranfection by electroporation were done by Newmann et al., Potter et al. and Fromm et al. [24-26] in the early 80s. Since then the number of research groups doing electroporation has increased dramatically.

Electroporation appears to be a promising method for integration on a chip, and is the focus of this thesis.

1.2.8.1 Mechanism of Electroporation

When a cell is exposed to a high intensity electric field pulse its cell membrane can be transiently permeabilized [27]. During this state of induced permeability, molecules can enter or exit the cell membrane. It is believed that the induction of a large transmembrane potential across the cell due to a high electric field is primarily responsible for the formation of pores. For a spherical cell with a radius, a, in a uniform electric field, E_0, the potential difference between the extracellular and intracellular surfaces of the cell is given by,

$$\Delta\Psi=1.5\, f a E_o \cos\theta[1-\exp(-t/\tau)]$$

$\tau = faC_m(r_i + r_e/2)$

$f = 1/[1 + a\ G_m(r_i + r_e)]$

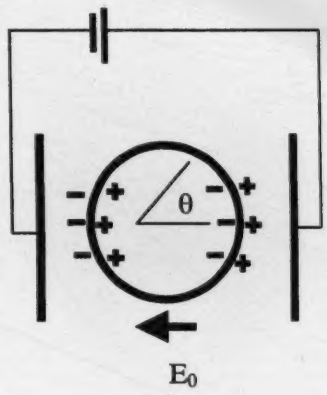

Figure 1.1 Induction of a transmembrane potential of a cell exposed to an electric field.

where, θ is the angle between the normal to the cell surface and the electric vector, as shown in figure 1.1, t is the time after the constant field is turned on, C_m is the membrane capacitance per unit area, r_i and r_e are the specific resistance for the intra and extracellular membranes, respectively, and G_m is the membrane conductance per unit area. For normal cells G_m is sufficiently small that f=1. When the induced potential $\Delta\Psi$ reaches a critical value it instigates an electrical breakdown of the cell membrane, creating pores. The value for $\Delta\Psi$ is typically 1 V. However, it can vary, depending on the pulse time and structure of the cell wall.

1.2.8.2 Electroporation of Bacterial Cells

The transfection of eukaryotic cells by electroporation had become an established method much before methods for bacterial cell electroporation were developed. Bacterial cells are more difficult to electroporate due to two fundamental differences. First, these cells are physically smaller in size than eukaryotes, and second, unlike eukaryotes, bacterial cells possess a thick cell wall, called the peptidoglycan. These two factors reduce the extent of pore formation. Bacterial cells must therefore undergo

electroporation under very high electric fields, typically 8-20 kV/cm, which reduces the cell viability after electroporation. Bacterial cells are generally divided into two classes, gram negative and gram positive, depending on their cell wall structure. Gram positive bacteria are harder to electroporate, due to an additional outer membrane within the cell wall. Despite these difficulties, electroporation is the best technique to introduce DNA into E.coli, although the efficiency of transfection varies from strain to strain. Transfection efficiencies of 10^{10} transfectants per μg have been reported in the literature [28]. In addition, more than 28 species of gram negative, and 40 species of gram positive bacteria have been transfected using electroporation [29]. A detailed review of these species is beyond the scope of this thesis, which for convenience, primarily focuses on the electroporation of a particular strain of E.coli (i.e. Dh5α).

1.2.8.3 Advantages of Bacteria Cell Electroporation

Although eukaryotic cell electroporation requires lower electric fields and is easier to achieve, bacterial electroporation techniques are less complicated. The advantages with bacteria are that; 1. protocols are simple, fast and inexpensive; 2. there is less reagent consumption; 3. recipient cells usually require no additional treatment; 4. cells can be easily cultivated and stored at –70°C; 5. highly purified plasmid DNA is not essential; 6. transfection may occur over a large plasmid concentration range; 7. for many species efficiency is independent of plasmid size; 8. electroporation is applicable to most gram negative and gram positive bacteria; 9. many commercial electroporators and auxiliary equipment are widely available; and 10. ample literature and established protocols already exist. Due to these many reasons, a bacterial cell line was selected for

this thesis which would ultimately pave the way for further experiments with mammalian cells.

1.2.8.4 Figures of Merit for Bacteria Electroporation

The primary figure of merit for electroporation is the transfection efficiency. Bacterial cells grow in vast numbers and are inexpensive, while DNA molecules are costly to prepare, so in determining the efficiency of transfection we express the results in terms of successful transformants per μg of plasmid DNA. That is, we determine how effectively the plasmid is consumed, rather than how effectively the cells are transfected. However, in order to obtain an estimate of the viability of cells upon electroporation, another term called the survival rate is commonly used. The survival rate is the percent of cells that are viable upon electroporation. Survival rates are more crucial to eukaryotic cell transfection than to bacterial cell transfection. Factors affecting the transfection efficiency are: 1. the type of cell and strain; 2. components of the growth media; 3. the size of the DNA, which may be limited to a maximum value; 4. in the case of electroporation the electrical parameters, including electric field strength and pulse time; 5. the effects of bacterial morphology, size, the state of aggregation and the plating techniques. These parameters are discussed in more detail in Chapter 3 (Sec 3.3.3).

1.2.8.5 Applications of Electroporation

The most widely used application of electroporation is gene transfer. This is achieved by incorporating DNA which contains a gene or genes of interest into the cell. In the case of bacterial cells, plasmids are the most common form of DNA used for insertion. The main chromosomes in bacteria contain about 4 million base pairs. In addition to this genetic material, bacterial cells also contain plasmids that are mobilizable,

small, circular molecules of DNA containing several thousand base pairs within the cytoplasm. These plasmids carry additional genes to convey desired characteristics, for example resistance to antibiotics such as ampicillin and tetracyclin. Genes present in plasmids can exist in large numbers because there can be many copies of a plasmid. Once a plasmid is transfected into a cell, the genes are expressed in the form of proteins. The expressed proteins can then be identified by different biochemical assays. When a cell is infected with a particular gene of interest, along with an antibiotic resistant gene, the cell upon expression of the genes can resist that particular antibiotic. Hence only cells that are successfully transfected survive growth in an antibiotic containing media. This method of incorporating antibiotic genes along with the gene of interest is a very useful way of monitoring cells that have been viably transfected.

A very important application of electroporation lies within the field of gene therapy, the technique of incorporating genes within chromosomes to cure genetic disorders. A majority of gene therapy techniques involve retroviral vectors for gene transfer. One disadvantage of retroviral vectors is they may cause mutational damage, leading to malignant transformation. In contrast, electroporation does not have this side effect, making it an indispensable tool for gene therapy. Reid and Smithies et al. [30] successfully used electroporation to incorporate genes into a mice germ line. Other applications include pollen electroporation for gene transfer in plants [31], electroporation of bacteria with plasmids [32], construction of plasmid libraries of higher than 10^9 recombinants [33], electroporation for protein injection into cell membranes [34], enzyme activity studies [35], etc.

In this thesis a microchip for electroporation was designed that utilized continuous flowing streams, with pressure driven flow. The electric field applied for electroporation induced electro osmotic flow. As a result, it is useful to review literature on microfluidic systems that utilize both of these pumping methods. Also, the general background on manipulating cells on chip provides a useful resource for the current project design and interpretation.

1.3 Electrokinetic μ-chip Devices – Recent Developments

Within the last few years there has been substantial development of the various individual components of μTAS devices. Electrokinetically driven devices capable of mixing, sample injection, multiple sample handling, on-chip preconcentration, filtering, DNA amplification, on-chip detection, etc, have been demonstrated in which many steps are integrated together [36]. The use of other materials besides glass, such as poly(dimethylsiloxane) (PDMS) [37] and polymethylmethacrylate (PMMA) [38] are being developed for chip fabrication. In spite of the fact that laser induced florescence (LIF) detection is still the number one form of detection, other systems like mass spectrometry and electrochemical detection [39,40] are becoming more popular.

The earliest microfluidic seperation devices consisted of a cross layout of a sample introductory channel and a separation channel connected to four reservoirs [41]. Two were for sample introduction and analysis buffer and the other two were for sample and buffer waste. However, in the last several years there has been a trend to fabricate more intricate microfluidic networks incorporating different functional steps. In order to efficiently mix reagent and sample within microfluidic devices, it is necessary to incorporate mixers within a microchannel network manifold. With electrokinetic

pumping as the driving force for fluid transport, reagents can be mixed in various proportions, depending on the geometry of the channels, applied electric fields and the material characteristics within the channel. Mixing on chip has already been accomplished by varying electric potential at the channel reservoirs to effect dilution [42], reactions [43,44], and solvent programming [45,46]. Harrison et al. were the first to show on-chip mixing [5], while Jacobson et al. were the first to perform parallel and serial mixing on a single microfluidic chip by means of a series of T-intersections [47]. The key element to designing an electrochemically driven mixing device is to fabricate the channels so as to simplify the voltage control required to obtain mixing. One of the most recent developments in mixers is an electrokinetic-instability micro mixer [48] that utilizes AC electric fields to efficiently mix. That work identifies certain instabilities in electrokinetic flow that are not understood yet.

A very important aspect of microfluidic devices is the need to fabricate devices that can produce well-defined reproducible injection plugs having good sensitivity and resolution within a separation channel. Different types of injectors such as T-injectors [41], double T-injectors [49] and cross injectors [50,51] have been used for on-chip capillary electrophoresis [41,49,50], micellar electrokinetic chromatography (MEKC) [52,53] and capillary electrophoresis. Alarie et al. [54] studied the effect of electric fields during sample loading and sample dispensing within a cross injector. Their findings concluded that within a cross injector the sample plug length can be controlled by both injection and separation voltages. In another study by Shultz-Lockyear et al. [55] electric field effects, injector geometry and sample matrix were described for a double T injector. The results demonstrated that long injection times result in reproducible sample plugs but

instabilities were observed. Also, the same ionic strength and pH for both sample and buffer produced most predictable results, with strong instability seen when compositions were not similar.

There has been significant improvement in the performance of microfluidic chips operating with EOF or with pressure driven flow. However, little has been done to fabricate and investigate systems that utilize EOF and pressure driven flow simultaneously. Pressure driven Poiseuille flow effects may arise within microfluidic channels due to the use of different ionic strength solutions within a channel network manifold [56]. These effects can be viewed by imaging, however the nature of such effects are very complicated and require theoretical modeling to be explained. J. G. Santiago investigated electro osmotic flow in microchannels associated with finite inertial and pressure forces [57]. He concluded that the velocity field in microchannels can be separated into inner and outer flow regions. Within the inner flow region (the electric double layer zone) fluid dynamics is dominated by the opposition of viscous and electrostatic forces, while that in the outer flow region (the bulk fluid) is dominated by pressure, inertia and non uniform surface charge. These conclusions provide mathematical justifications for these commonly applied conclusions. Simultaneous application of EOF and pressure driven flow has recently been used in capillary electrochromatography [58]. In such systems resolution of separation can be increased by adjusting the ratio of the pump pressure and separation voltage [59]. Qin-Hua Ru et al. [60] showed that reversed pressure in pressurized capillary electrochromatography could increase repeatability while larger forward pressures could decrease separation times. However, in both cases the main driving force for separation is electrophoresis.

These various studies indicate the interest in considering EOF and pressure driven flows is increasing, but a full understanding has not yet emerged.

1.4 Electro Osmotic and Pressure Driven Flow Systems

Electro osmotic flow (EOF) is an electric field induced phenomena that is responsible for fluid propulsion within small capillaries. It arises due to the surface charge on the capillary wall. Pressure driven flow systems on the other hand generate fluid propulsion due to a pressure drop. Both of these systems have been used extensively for fluid manipulation within microfluidic devices. The next few sections discuss the nature and properties of EOF and pressure driven flow.

1.4.1 Generation of EOF in Capillaries - The Double Layer Theory

The surface of fused silica capillaries contains many silanol (Si-OH) groups. At pH values greater than 4 these groups may be deprotonated, resulting in a negatively charged surface. To preserve charge neutrality, positive ions are in excess in solution near the surface of the wall. This layer of charge is known as the compact Helmholtz or Stern layer. Ions in the Stern layer are usually not solvated. The plane going through the centre of charges in this layer is known as the inner Helmholtz plane (IHP). Outside the IHP, hydrated positive ions approach the capillary wall up to a certain distance. At this distance the plane going through the centers of the hydrated positive ions is known as the outer Helmholtz plane (OHP). The negative layer of charge on the wall along with the positive layer of non-hydrated and hydrated ions next to it is known as the electric double layer. It is shown in Figure 1.2. The potential difference between the plane of shear that is in the vicinity of the OHP, and the capillary wall is known as the zeta potential, ζ. The

solvated positive ions outside the OHP constitute the diffuse layer. The thickness of the diffuse layer can be expressed as the reciprocal of the Debye layer thickness, i.e.,

$$\frac{1}{\kappa} = \sqrt{\frac{\varepsilon KT}{2000e^2 NI}}$$

where ε is the permitivity of the electrolyte, K is Boltzman's constant (1.38×10^{-23} JK^{-1}), T is the absolute temperature (K), e is the charge of an electron (1.6×10^{-19} C), N is Avagadro's constant (6.023×10^{23}) and I the ionic strength [M]. Ions in the diffuse layer are non-specifically absorbed to the surface and are mobile compared to ions closer to the wall due to thermal agitation and decreased extent of electrostatic interaction. When an electric field is applied across the capillary, hydrated positive ions

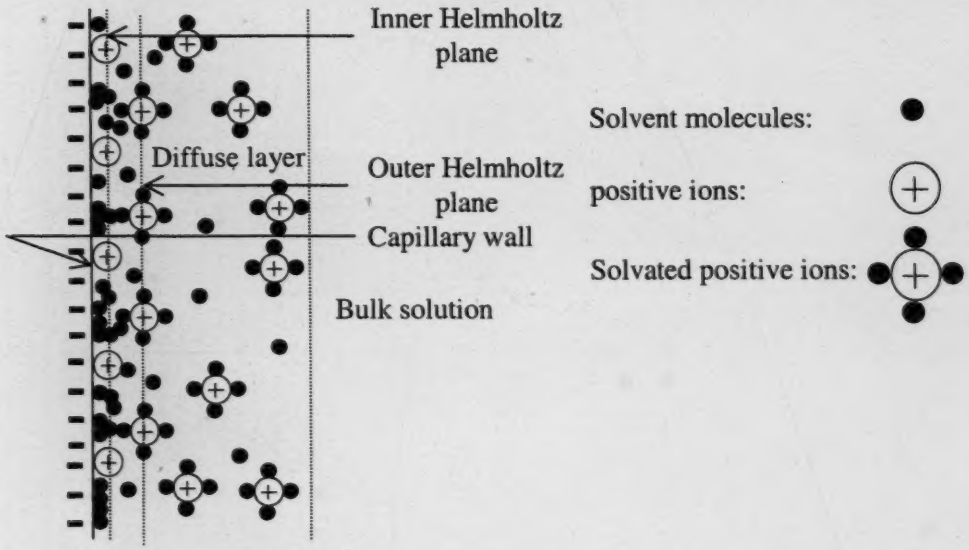

Figure 1.2 The diffuse double layer.

within the diffuse layer migrate towards the cathode, dragging solvent molecules along due to friction. This causes a bulk flow of solution within the capillary known as electro osmotic flow (EOF). The magnitude of EOF can be expressed in terms of mobility or velocity. The linear velocity due to EOF is given by $v_{eof} = \mu_{eof} \times E$, where μ_{eof} is the EOF

mobility and E is the electric field. The EOF mobility is given by, $\mu_{eof} = \varepsilon\zeta/(4\pi\eta)$, where η is the viscosity of the solution

1.4.2 Factors Influencing EOF

EOF is useful in capillary electrophoresis (CE) separations, since it causes all ions to move in one direction. However, in many instances it is necessary to modify the EOF. This may be accomplished by changing the surface properties of the capillary wall or by changing the properties of the bulk solution. There are quite a number of factors that have an influence on EOF. Table 1.1 lists these properties and their affects on EOF.

Table 1.1 Factors influencing EOF

Factors effecting EOF	**Consequences**
Electric Field	EOF is proportional to electric field.
Ionic strength	Increased ionic strength decreases the zeta potential leading to a loss in EOF.
Buffer pH	Zeta potential and EOF is reduced at low pH(<4) and increased at high pH
Temperature	Changes viscosity 2-3% per °C. EOF increases with temperature.
Organic modifier	Changes viscosity and zeta potential. Reduction in EOF.
Coating on wall	Can increase, decrease or eliminate EOF depending on the surface chemistry.

1.4.3 Pressure Driven Flow

Many cell based microfluidic devices use pressure driven flow. It is therefore necessary to understand some details of Poiseuille flow. Unlike EOF, where flow is generated from the surface of the capillary wall, pressure driven flow results from the flow of liquid due to a pressure drop across the capillary. Pressure driven flow through a cylinder may be considered as a flow of concentric sheaths of liquid. The layer closest to the cylinder wall will produce the most frictional drag, making it stagnant. Layers deeper within the cylinder possess less frictional drag, making their velocities faster as they

move within the center of the cylinder, creating a velocity gradient. The velocity of the liquid in the center is the highest due to the least frictional drag. This is shown in Figure 1.3(a). This type of flow is called laminar flow or streamline flow. The flow profile for such a flow will be parabolic. The volumetric flow rate Q associated with laminar flow can be calculated by the Poiseuilles equation for a tube by $Q=\pi R^4(P_2-P_1)/8\eta L$, where R is the radius of the tube, (P_2-P_1) is the pressure drop, η is the viscosity of the solution and L is the length of the tube. Figure 1.3 shows the flow profiles for pressure driven flow and EOF. Unlike pressure driven flow, EOF has a plug profile. All the particles in an EOF profile move essentially at the same velocity.

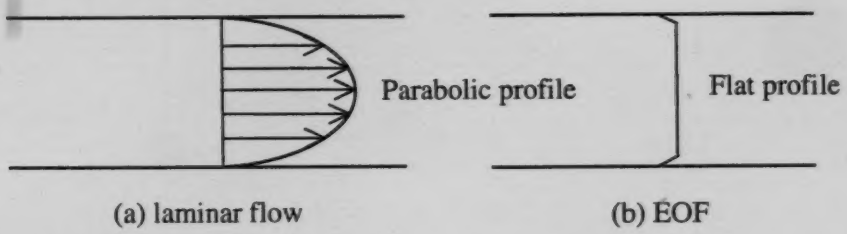

Figure 1.3 (a) Laminar flow profile for pressure driven flow. (b) Plug flow profile for EOF

1.5 Cells on a Chip: An Overview

In considering research on an electroporation chip it is worthwhile to evaluate previous efforts to work with cells on chip. One of the more novel applications of microfluidic devices is its potential use as a tool to perform biological functions on chip with cells. Applications of cells on a chip include cell transport, mechanical and chemical manipulation, sorting, lysing, cultures, etc. More recent developments include the investigation of different cellular processes. In order to accomplish these goals, cells on microchips have been manipulated both with EOF and pressure driven flow. Microfluidic chips possess features on a size scale compatible to that of cells. It is therefore very practical to be able to manipulate cells in such devices. Li, P. et al. [56]

fabricated a microfluidic system that enabled the mobilization of cells within a network of channels followed by lysis of the cells using a detergent. The results demonstrated that different types of cells could be precisely manipulated within certain structures on chip using electro osmotic pumping. In addition it is also possible to manipulate larger cellular structures such as embryos within microfluidic channels. In order to improve efficiencies in assisted reproduction, D. Beebe et al. [62] in their research fabricated a microfluidic chip to perform loading/unloading of oocyte/embryo, on-chip chemical and mechanical manipulation and testing for viability. The removal of the zona pellucida by acid treatment demonstrated successful chemical treatment while the removal of cumulus cell from an embryo by suction demonstrated mechanical manipulation. Ian K Glassgow et al. [63] showed in their work that mammalian embryos can be incorporated into microfluidic devices, retained in specific chambers and extracted safely. Embryo development is normal within such devices.

Examples of cell culture on-chip include the culture of army worm ovaries on PDMS chips [64], fabrication of devices to contain cultures that do not need surface modification of substrate prior to seeding [65], investigation of the non-genetic variability cell-division cycle and growth of Ecoli cells within pico liter sized microcages [66], incubation of Ecoli expressing GFP [67], etc. Manipulation of cell organelles using optical tweezers was first achieved by Aaron R. Wheeler et al. [68]. Another striking example of cell manipulation using optical tweezers involves the work of Günter R. Fuhr [69] in which single cells are isolated for diagnostic assays. A lot of the current research into cells on a chip involves the investigation of cellular behavior in microscopic environments. Kricka and Wilding [70] fabricated a chip for semen analysis, in vitro

fertilization, PCR and immunoassay. These chips were used to determine sperm mobility. Sperm were selected on-chip and used to fertilize an egg in a separate chamber. Successful fertilization followed by growth from a two cell zygote to a blastocyste was demonstrated. Microchannels simulating human blood capillaries have been utilized to investigate the flow behavior of erythrocytes [71]. Capillaries micromachined in silicon enabled the application of physiological pressures and temperatures while real time imaging processing allowed continuous monitoring of cells. Similar studies investigating blood cell deformability have also been conducted [72]. Other blood related research on chips involve blood sample preparation and PCR [73]. The most challenging aspect of research with cells on chip is perhaps the ability to integrate several biological functional steps, in order to build a total analysis system which would produce a final product through a series of biological events occurring within a single device. A lot of the present microfluidic cell research is therefore geared towards integration of such steps along with miniaturization.

1.6 The Scope of this Thesis

Gene transfection is a crucial tool for researchers to explore the field of molecular biology, genomics and recombinant DNA technology. However, present protocols to perform gene transfection are somewhat laborious, time consuming and not automated. Our goal was to fabricate a microfluidic device that could perform electroporation for gene transfection to demonstrate its potential as an individual biological functional step. Coupled to other on-chip biological processes it could prove to be a useful tool in the automation of biological laboratory research.

Chapter 2 gives a detailed description of the geometric factors of channels that influence electric field and volumetric flow. The calcium uptake experiments using fluorescence detection and initial transfection experiments are also described.

Chapter 3 describes the rationale behind the fabrication of a redesigned single channel Electroporation chip. Electroporation and chip specific parameters are discussed in detail followed by studies on pulse times, electric fields, cell and DNA concentrations, etc.

Chapter 4 deals with the conclusions from the previous chapters and future development.

1.7 References

1. Graber, N.; Lüdi, H.; Widmer, H. M. *Sens. Actuators B* 1990, 1, 239.
2. Manz, A.; Graber, N.; Widmer, H. M. *Sens. Actuators B* 1990, 1, 244.
3. Garn, M.; Cevy, P.; Gisin, M.; Thommen, C. *Biotechnol. Bioeng.* 1989, 34, 423.
4. Terry, S. C.; Jerman, J. H.; Angell, J. B. *IEEE Trans. Electron. Devices* 1979, ED26, 1880.
5. Harrison, D. J.; Flur, K.; Seiler, K.; Fan, Z.; Effenhauser, C. S.; Manz, A. *Science* 1993, 261, 895-897.
6. Shi, Y.; Simpson, P. C.; Scherer J. R.; Wexler, D.; Skibola, C.; Smith, M. T.; Mathies, R. A. *Anal. Chem.* 1999, 7, 5354-5361.
7. Vaheri, A.; Pagano, J. S. *Virology* 1965, 27, 434.
8. Graham, F. L.; van der Eb, A. J. *Virology* 1973, 52, 456.
9. Felgner, P. L. *Proc. Natl. Acad. Sci. USA* 1987, 84, 7413.
10. Grandgenett, D. P.; Mumm, S. R. *Cell* 1990, 60, 3.
11. Burkholder, J. K.; Decker, J.; Yang, N. S. *J. Immunol. Methods* 1993, 165, 149.
12. Capecchi, M. R. *Trends Genet.* 1989, 5, 70.
13. Tang, M. X.; Szoka, F. C. Gene Therapy 1997, 4, 823.
14. Tang, M. X.; Redemann, C. T.; Szoka Jr, F. C. *Bioconjugate Chem.* 1996, 7, 703.
15. Cole, K. S. *A Chapter of Classical Biophysics*, University of California press, Berkeley, 1968, pp-12-18.
16. Sale, A. J.; Hamilton, W. A. *Biochim. Biophys. Acta* 1967, 148, 781-800.
17. Crowley, T. M. *Biophys. J.* 1973, 13, 711-724.
18. Zimmermann, U.; Pilwat, G.; Riemann, F. *Biophys. J.* 1974, 14, 881-889.

19. Neumann, E.; Rosenheck, K. J. *Membrane Biol.* 1972, 10, 279-290.

20. Kinosita, K.; Tsong, T. Y. *Proc. Natl. Acad. Sci.*1977, 74, 1923-1927.

21. Baker, P. F.; Knight, D. E. *J. physiol.* 1978, 284, 30.

22. Zimmermann, U.; Vienken, J.; Pilwat, G. *J. Electroanal. Chem.* 1980, 116, 553-574.

23. Knight, D. E.; Baker, P. F.; *J. Membrane Biol.* 1982, 68, 107-140.

24. Neumann, E.; Schaefer-Ridder, M.; Wang Y.; Hofschneider, P. H. *EMBO J.* 1982, 1, 841-845.

25. Potter, H.; Weir, L.; Leder, P. *Proc. Natl. Acad. Sci. USA* 1984, 81, 7161-7165.

26. Fromm, M. L.; Taylor, P.; Walbot, V. *Nature* 1986, 319 791-793.

27. Benz, R.; Zimmermann, U. *Biochim. Biophys. Acta.* 1981, 640, 169-178.

28. Dower, W. J.; Miller, J. F.; Ragsdale C. W. *Nucleic Acids Res.* 1988, 16, 6127-6145.

29. Chang, D. C.; Chassy, B. M.; Saunders, J. A.; Sowers, A. E. *Guide to Electroporation and Electrofusion*, Academic Press Inc., San Diego, 1992, p-271

30. Reid, L. H.; Sheseley, E. G.; Kim, H. S.; Smithies, O. *Mol. Cell Biol.* 1991, 11, 2769-2777.

31. Abdul-Baki, A. A.; Saunders, J. A.; Matthews, B. F.; Pittarelli, G. W. *Plant Sci.* 1990, 70, 181-190.

32. Bolivar, F.; Backman, B. *Methods in Enzymology* 1979, 68, 245-267.

33. Cwirla, S. E.; Peters, E. A.; Barret, R. W.; Dower, W. J. *Proc. Natl. Acad. Sci. USA* 1990, 87, 6378-6382.

34. Mouneimne, Y; Tosi, P. F.; Barhoumi, R.; Nicolau, C. *Biochim. Biophys. Acta.* 1991, 1066, 83-89.

35. Swezey, R. R.; Epel, D. *Cell Regul.* 1989, 1, 65-74.

36. Bruin, G. J. M. *Electrophoresis* 2000, 21, 3931-3951.

37. Effenhauser, C. S.; Bruin, G. J. M.; Paulus, A.; Ehrat, M. *Anal. Chem.* 1997, 69, 3451-3457.

38. Ford, S. M.; Kar, B.; McWhorter, S.; Davies, J.; Soper, S. A.; Klopf, M.; Calderon, G.; Saile, V. *J. Microcol. Sep.* 1998, 10, 413-422.

39. Woolley, A. T.; Lao, K.; Glazer, A. N.; Mathies, R. A. *Anal. Chem.* 1998, 70, 684-688.

40. Li, J.; Thibault, P.; Bings, N. H.; Skinner, C. D.; Wang, C.; Colyer, C. L.; Harrison, D. J. Anal. Chem. 1999, 71, 3036-3045.

41. Harrison, D. J.; Manz, A.; Fan, Z.; Lüdi, H.; Widmer, H. M. *Anal. Chem.* 1992, 64, 1926-1932.

42. Culbertson, C. T.; Ramsey, R. S.; Ramsey, J. M. *Anal. Chem.* 2000, 72, 2285-2291.

43. Hadd, A. G.; Raymond, D. E.; Halliwel, J. W.; Jacobson, S. C.; Ramsey, J. M. *Anal. Chem.*1997, 69, 3407-3412.

44. Salimi-Moosavi, H.; Tang, T.; Harrison, D. J. *Am. Chem. Soc.* 1997, 119, 8716-8717.

45. Kutter, J. P.; Jacobson, S. C.; Ramsey, J. M. *Anal. Chem.* 1997, 69, 5165- 5171.

46. Kutter, J. P; Jacobson, S. C.; Mastubara, N.; Ramsey, J. M. *Anal. Chem.*1998, 70, 3291-3297.

47. Jacobson, S. C.; Mc Knight, T. E.; Ramsey, J. M. *Anal. Chem.* 1999, 71, 4455-4459.

48. Oddy, M. H.; Santiago J. G.; Mikkelson, J, C. *Proceedings of the m-TAS 2001 Symposium*, Monterey, p-

49. Effenhauser, C. S.; Manz, A.; Widmer, H. M. *Anal. Chem.* 1993, 65, 2637-2642.

50. Jacobson, S. C.; Hergenröder, R.; Koutny, L. B.; Warmack, R. J.; Ramsey, J. M. *Anal. Chem.* 1994, 66, 1107-1113.

51. Jacobson, S. C.; Hergenröder, R.; Moore Jr, A. W.; Ramsey, J. M. Anal. Chem 1994, 66, 4127-4132.

52. Moore Jr, A. W.; Jacobson, S. C.; Ramsey, J. M. *Anal. Chem.* 1995, 67, 4184-4189.

53. Van Heeren, F.; Verpoorte, E.; Manz, A.; Thormann, W. *Anal. Chem.* 1996, 68, 2044-2053.

54. Alarie, J. P.; Jacobson, S. C.; Culbertson C. T.; Ramsey, J. M. *Electrophoresis* 2000, 21, 100-106.

55. Shultz-Lockyear, L. L.; Colyer, C. L.; Fan Z. H.; Roy, K. I.; Harrison, D. J. *Electrophoresis* 1999, 20, 529-538.

56. Lichtenberg, J.; Verpoorte, E.; De-Rooj, N. F. *Electrophoresis* 2001, 22(2), 258-271.

57. Santiago, J. G.; *Anal. Chem.* 2001, 73, 2353-2365.

58. Tsuda, T. *Anal. Chem.* 1988, 60, 1677.

59. Eimer, T.; Unger, K. K.; Van Der Greef J. *Trends Anal. Chem.* 1996, 519, 463.

60. Ru, Q.; Luo, G.; Fu, y. *J. Chromatogr.* A 2001, 924, 331-336.

61. Li, P.; Harrison, D. J. *Anal. Chem.* 1997, 69, 1564-1568.

62. Beebe, D.; Wheeler, M. B.; Zeringue, H. C.; Walters, E.; Raty, S. *Theriogenology* 2002, 57, 125-135.

63. Glasgow, I. K.; Zeringue, H. C.; Beebe, D. J.;Choi, S.; Lyman, J. T.; Chang, N. G.; Wheeler, M. B. *IEEE Trans. Biomed. Eng.* 2001, 48, 570-577.

64. Walker, G. M.; Ozers, M. S.; Beebe, D. J. *Biomed. Microdevices* 2002, 4(3), 161-166.

65. Folch, A.; Jo, B. H.; Hurtadu, O.; Beebe, D. J.; Toner, M. J. *Biomed. Materials Research* 2000, 52(2), 346-353.

66. Inoue, I.; Wakamoto, Y.; Yasuda, K. *Proceedings of the Japan Academy Series B Physical and Biological Science* 2001, 77(8), 145-150.

67. Monaghan, P. B.; Manz, A.; Nichols, W. W. *Proceedings of the Micro TAS 2000 symposium*, Netherlands, p-111.

68. Wheeler, A. R.; Morishima, K.; Arnold D. W.; Rossi, A. B.; Zare, R. N. *Proceedings of the Micro TAS 2000 symposium*, Netherlands, p-25.

69. Fuhr, G. R.; Reichle C. *Proceedings of the Micro TAS 2000 symposium*, Netherlands, p-261

70. Kricka, L. J.; Wilding, P. *Pure and Applied Chem.* 1996, 68(10), 1831-1836.

71. Sutton, N.; Tracey, M. C.; Johnston, I. D.; Greenaway, R. S.; Rampling, M. W. *Microvascular* Research 1997, 53(3), 272-281.

72. Tracey, M. C.; Greenaway, R. S.; Das, A.; Kaye, P. H.; Barnes, A. J. *IEEE Trans Biomed. Eng.* 1995, 42(8), 751-761.

73. Yuen, P. K.; Kricka, L. J.; Fortina, P.; Panaro, N. J.; Sakazume, T.; Wilding, P. *Genome Research* 2001, 11(3), 405-412.

Chapter 2: DNA Transfection of E. coli Using a Microfluidic Chip

2.1 Introduction

Since its inception less than 25 years ago electroporation has become the method of choice for cell transfection in many instances, due to its applications in molecular and cellular biology. Electroporation is more of a physical phenomenon than a biochemical one, making it a widely applicable technique. It has been successfully performed on all types of cells: animal, plant and microbial [1-3]. It causes less perturbation to cells minimizing genetic deformity associated with cloning and other recombinant DNA techniques.

Developing biological applications for microfluidic chips is becoming more popular day by day. Along with a variety of on-chip biological processes it would be very useful to perform electroporation on-chip for future applications in molecular biology techniques. Coupled to other on-chip biological functional steps, electroporation could be a part of an integrated system aimed towards automation and faster performance of conventional biomolecular techniques. Because a major portion of microfluidic devices utilize a continuously flowing stream, our goal was to explore the possibility of performing electroporation within a continuous flow process. In order to do so, we required a microfluidic chip capable of providing an electroporation zone which could provide a strong enough electric field. The fluid paths need to be designed to not leak too much liquid from the porator zone into the voltage delivery channels. We ultimately fabricated an initial prototype design that enabled us to test Ca ion uptake and DNA transfection within E.Coli DH5α bacteria cells.

2.2 Experimental

2.2.1 Device Fabrication and Instrumentation

Microfluidic chips were fabricated on 4 inch square Corning 0211 glass plates, with access holes drilled through cover plates, as previously described [4,5]. The weir design required use of a two-mask process, in which weirs were etched 3 μm deep and the remaining channels were 20 μm deep. Figure 2.1 shows the layout of the chip, and indicates the labeling scheme used. Cells were pumped through the chip using a syringe pump (PHD 2000, Harvard Apparatus, Holliston, MA, U.S.A) fitted with a gas tight syringe (SGE syringe, gastight 100 µL RN, 25ga, Pt#2, Austin, TX, USA), connected with PEEK tubing (0.06" OD, 0.005" ID, SPE Ltd., Concord, ON, Canada) using a flangeless screw fitting (P-200X, SPE Ltd.) to seal at reservoir A, with the chip mounted in a plexiglass holder. Voltages were applied

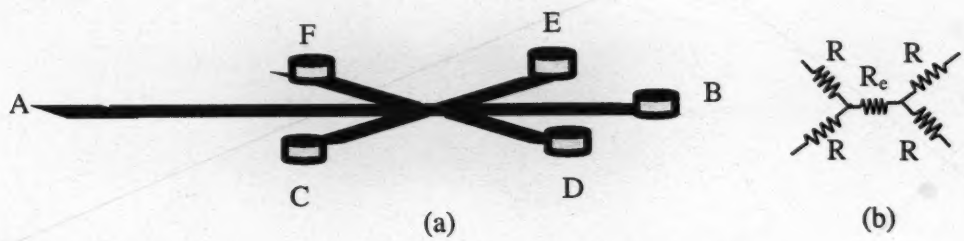

Figure 2.1 (a) Sketch of chip showing labeling scheme. (b) Equivalent electrical circuit.

to reservoirs C-F with Pt electrodes. The potential was applied through a high voltage relay (30 KV, double-throw, Kilovac, Santa Barbara, CA, USA), with both the power supply and the relay under the control of a MacIntosh Power PC 7100/66 through an NB-MIO-16H board (National Instruments, TX, USA). Voltages were applied in a pulse train with a 50 % on/off duty cycle, controlled by switching the relay. A homebuilt confocal, epiluminescent microscope with a 40 x objective was mounted below the chip for fluorescence detection, and another homebuilt microscope with a 25 x objective was

mounted above for visual observation with a 10 x eyepiece or a CCD camera (Sony, model#SSC-C370). An R1477 Hamamatsu photomultiplier tube (PMT) coupled with a 515nm fluorescence filter (Omega Optical, Brattleboro, VT) were used for fluorescence detection.

2.2.2 Cell Growth and Preparation

All experiments were conducted using the same strain of bacteria, E. Coli DH5α, to produce electrocompetant cells. One litre of fresh LB broth (10 g tryptone, 5 g yeast and 10 g NaCl dissolved to 1 litre and adjusted to pH 7.2 using 1 M NaOH followed by autoclaving) was innoculated with the bacteria directly from a new vial with an innoculating loop. The culture was allowed to grow overnight in a shaker (Innova 4330, New Brunswick Scientific) at 250 rpm and 37 °C to an optical density (OD) of 0.9-1.1. After 15 hours of culture the OD was monitored on a UV-Vis spectrometer at 600 nm by taking 2 mL aliquots with sterile pasture pipettes from the culture every 30 minutes until the desired OD was attained. Cells were then chilled on ice and transferred to chilled centrifuge tubes (Beckman, 250 mL) and centrifuged at 4 °C for 15 min at 5000 rpm with a Beckman centrifuge (model# J2-21). The cells were washed with 250 mL ice cold dd H_2O and spun down 3 times using the same conditions, followed by washing with 30 mL sterilized 10% glycerol using the same spinning conditions. Finally the cells were resuspended in 30 mL 10% sterilized glycerol. One mL aliquots were transferred to eppendorf tubes on ice and stored at –70 °C in the freezer. Each tube was thawed on ice before each experiment. In order to determine the cell concentration a tube was thawed and a series of dilution steps were performed to reduce the cell concentration 10^7 fold, then a 100 µL aliquot of this solution was spread on to a culture plate (100 x 15 mm,

Fischer brand) filled with agar. The number of colonies was then easily counted and the initial cell concentration was calculated based upon the dilution factor. The cell concentration in the glycerol stock was estimated to be 1.7×10^9 cells/mL.

To detect fluorescence signal from the cells upon electroporation, the cells were loaded with Fluo-4 dye (Flùo-4 AM, Molecular Probes). Cells previously stored were thawed on ice and a 50 μL aliquot was diluted to 500 μL with 5 mM fluo-4 dye in 5 mM borate buffer, adjusted to pH 8.0 with 1 M HCl. The cells were transferred to a shaker operated at 250 rpm and 37 °C for 20-30 min. Upon penetration of the dye within the cells, 3 cycles of washing with 5 mM borate buffer were performed using a centrifuge operated at 4000 rpm for 2 minutes, to remove the excess dye. The cells were then resuspended in 5 mM borate buffer and were brought to a volume of 500 μL. This corresponded to a cell concentration of 1.7×10^8 cells/mL. This solution was loaded into a syringe and used for further experiments.

In order to perform transfection experiments with plasmids, a stored vial of cells was thawed on ice and 100 μL of the cells was diluted to 1 mL using dd H_2O. 160 μL of this solution was transferred to an Eppendorf tube in which 2 μL of 500 ng/μL plasmid was added and mixed with the flick of a finger. This cell solution was used for the transfection experiments. Cells flowing through the channel at 1 μL/min were exposed to 75 pulses with a 50% duty cycle and 1 s period. Having performed the transfection experiments the cells were collected from the cell-receiving reservoir, diluted with LB broth, plated and screened for colonies. Culture plates were prepared with 25 mL aliquots of LB agar (10 g tryptone, 5 g yeast and 10 g NaCl, dissolved to 1 litre and adjusted to pH 7.2 using 1 M NaOH followed by addition of 15 g bacto agar and

autoclaving for 20 minutes) which was then poured into each plate. Prior to pouring, ampicillin was added to the media to give a final concentration of 50 mg/L. X-gal was dissolved in dimethylformamide (DMF) to a concentration of 20 mg/mL. 40 μL of X-gal and 100 μL of 40 mM isopropylthio-beta-D-galactoside (IPTG) was spread on to the plates 30 minutes prior to plating.

2.2.3 Chip Operation

To detect fluorescence signal from the cells upon electroporation the cells were loaded with Fluo-4 dye. To determine electroporation conditions Fluo-4 loaded cells were introduced to reservoir inlet A (Figure 1) and pumped downstream into a cross section containing Ca^{2+} ions. The cell concentration was 1.7 x 10^8 cells/mL. The Ca^{2+} concentration at the four reservoirs C,D,E and F was kept at 5 mM in 5 mM borate buffer. High voltage pulses ranging from 500 V-1500 V were applied through the cross region. Reservoirs D and E were connected to the positive potential while F and C were at ground. A PMT/CCD detection scheme at the cross region was used to monitor the fluorescence due to the formation of Fluo-4-Ca^{2+} complex within the cells after electroporation. The pump was set to deliver a flow rate of 1 μL/min.

For transfection experiments, cells in a plasmid loaded solution were pumped at 1 μL/min from point A to B. The plasmid concentration was 6.17 ng/μL. The direction of the EOF was changed by changing the polarity of the electrodes. The cells were exposed to 75 pulses with a 50% duty cycle and 1 s period. Having completed the pulses, cells were collected from reservoir B with a pipette, in a volume of about 100 μL, and diluted to 300 μL. 100 μL of this solution was plated on ampicillin agar plates containing X-gal and IPTG. Transfection efficiency was determined by counting the number of colonies on

the plate, directly or under UV light, depending on the type of plasmid used, and calculating the number of transfectants per μg of plasmid. A dilution of 1.2 μL of cells in 100 μL of the reservoir volume does not affect the calculation to obtain transfection efficiency because the total volume of cells was collected for subsequent analysis.

2.3 Results and Discussion

2.3.1 Device Design

The star shaped intersection illustrated in Figure 2.1 was created to provide an electroporation zone for cells in a moving stream. The device was designed to use pressure driven flow to deliver a stream of cells along a straight channel through the electroporation zone, where a high strength electric field could be applied to induce pore formation. A relatively uniform electric field was created within the zone, by applying voltages to the four reservoirs; a high voltage on reservoirs F and C (Figure 2.1 a) and a low voltage on reservoirs D and E or vice-versa. In order to reduce pressure driven flow within the side channels, weirs were etched 3 μm deep, creating a higher resistance to flow relative to the 20 μm deep main channel in which the cells were pumped. Figure 2.2 shows a schematic diagram of a side arm of the cross region. The electrical impedance of the side channels relative to the eletroporation zone is also important to device performance, as it dictates the percentage of applied field that drops within the zone. Figure 1b shows an equivalent circuit model of the relevant segments of the device.

2.3.1.1 Detailed Analysis of Geometric Effects on Electric Field and Flow

The weirs in the hydrochip act as a resistance to cells flowing into reservoirs C,D,E and F. This whole network of channels may be considered as an equivalent set of electric resistors and can be mathematically simplified to calculate the electric field

strength within the mid section of the cross region, i.e., the electroporation zone. Figure 2.1(b) shows the electrical equivalent of the chip. The resistance of any one of the four identical side channels, including the weir is R, where

$$R = \rho \sum_i \frac{l_i}{A_i} \tag{2.1}$$

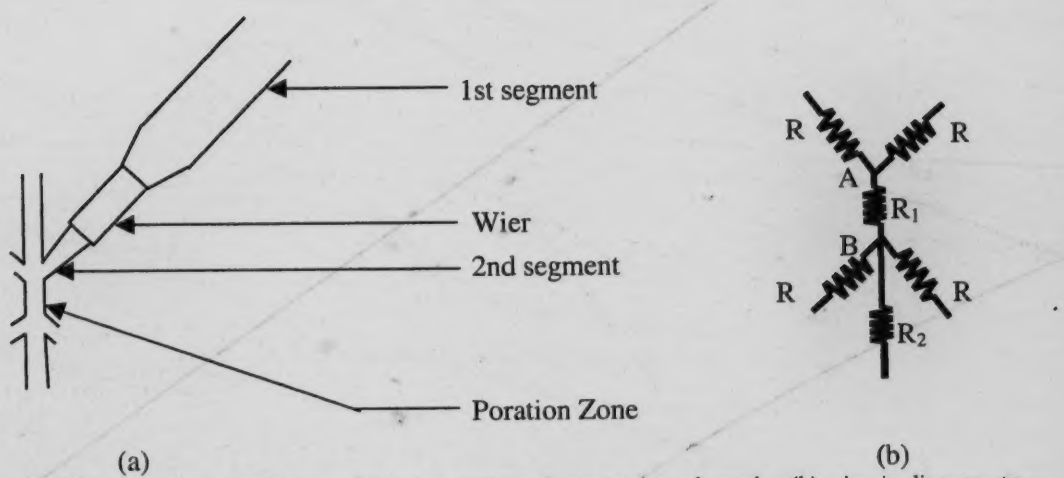

Figure 2.2 (a) Diagram of side arm showing weir and connecting channels. (b) circuit diagram to determine resistance to flow.

Table 2.1 Dimensions for different sections of the hydro chip.

3 μm weir device	Length (μm)	Depth (μm)	Width (μm)	F
Segment 1	5580	20	240	0.0263
Weir	120	3	66	0.0147
Segment 2	210	20	50	0.0997
Poration zone	150	20	50	0.0997
Post poration zone	14000	20	50	0.0997
1 μm weir device	Length (μm)	Depth (μm)	Width (μm)	F
Segment 1	5580	20	240	0.0263
Weir	120	1	62	0.0053
Segment 2	210	20	50	0.0997
Poration zone	150	20	50	0.0997
Post poration zone	14000	20	50	0.0997

and l_i is the length of the channel segment i, A_i is the cross section of the segment and ρ is the resistivity of the solution. Similarly

$$R_e = \rho \frac{l_e}{A_e} \tag{2.2}$$

where l_e and A_e are the dimensions of the electroporation zone. After simplifying the circuit in figure1(b) it can be shown that the fraction of the voltage drop across the electroporation zone is $\frac{R_e}{R + R_e}$ (2.3)

Hence the voltage across the electroporation zone is

$$V = \frac{R_e}{R + R_e} V_T \tag{2.4}$$

where V_T is the total applied voltage. The electric field strength useful for electroporation is then

$$E = \frac{V}{l_e} \tag{2.5}$$

The values for R and R_e can be calculated from the chip's geometrical parameters listed in Table 2.1. For the hydrochip we have

$$R = \left(\frac{5580}{20 \times 240} + \frac{120}{3 \times 60} + \frac{210}{20 \times 50} \right) \rho \quad \text{.....from Equation 2.1 and}$$

$$R_e = \frac{150}{20 \times 50} \rho \quad \text{.....from Equation 2.2}$$

From Equation 2.3 it was calculated that 7.04 % of the applied voltage drop occurred within the electroporation zone.

In order to determine fluid resistance within the channels, similar calculations involving the channel dimensions were used. The average linear flow rate v in a rectangular channel [6] can be expressed by

$$v = \frac{\phi}{A} = \frac{wd\Delta PF}{4\eta L} \tag{2.6}$$

where, w, d and L are the width, depth and length of the channel, respectively, ΔP is the pressure difference, η the viscosity, F is a geometrical form factor (see Section 3.2.2.2), ϕ is the volumetric flow rate and A is the cross sectional area of the channel. Equation 2.6 can be rearranged to

$$\Delta P = \phi \left(\frac{4\eta L}{(wd)^2 F} \right) \tag{2.7}$$

The volumetric flow in a channel can be compared to the current through a conductor so that the pressure difference in the channel is equivalent to the potential difference.

According to Kirchhoff's law, voltages in a circuit are additive and there is no accumulation of charge at junctions during current flow. Similarly, pressure drops are additive and there is no accumulation of mass at junctions during volumetric flow. The right hand side of Equation 2.7 in brackets may therefore be considered as equivalent to electrical impedance. Therefore the impedance for a volumetric channel can be expressed by

$$r = \frac{4\eta L}{(wd)^2 F} \tag{2.8}$$

To determine the resistance to flow within the channels we use a circuit diagram similar to that used for electric field shown in Figure 2.2(b). In order to evaluate the fraction of flow leaking through the first set of weirs at point A, we compare,

$$R_1 + \left(\frac{1}{R_2} + \frac{1}{R/2} \right)^{-1} \quad \text{vs} \quad R/2$$

where R_1 is the fluid resistance for the electroporation zone, R_2 is for the main channel downstream of the zone and R is for any of the side channels. To evaluate the leakage at the second set of weirs we compare,

$$R_2 \quad \text{vs} \quad R/2$$

The values for R, R_1 and R_2 are calculated as follows from the geometrical parameters in Table 2.1,

$$R = \left(\frac{4 \times 5580}{(240 \times 20)^2 \times 0.0263} + \frac{4 \times 120}{(66 \times 3)^2 \times 0.0147} + \frac{4 \times 210}{(50 \times 20)^2 \times 0.0997} \right) \eta \ \mu m^{-3}$$

$$R_1 = \frac{4 \times 150}{(50 \times 20)^2 \times 0.0997} \eta \ \mu m^{-3}$$

$$R_2 = \frac{4 \times 14000}{(50 \times 20)^2 \times 0.0997} \eta \ \mu m^{-3}$$

It is calculated that 36.5% of the flow leaks into the first set of weirs and 35.6.% at the second set. Calculations from Table 2.1 for a 1 μm weir device show that the overall leakage is only 8.9% and the fraction of voltage drop across the weir is 4.34%. This device would therefore be expected to perform better than the 3 μm weir device due to less leakage, resulting in more efficient use of the plasmid. However, at the same time, a lower fraction of voltage drop across the electroporation zone would prevent us from attaining higher electric fields. Regardless, our attempts at using a 1 μm device failed due to plugging of the weirs.

In order to determine the pulse time, T_{por} (i.e. time for the cells to cross the electroporation zone), the total linear velocity within the poration zone had to be determined first. Due to the fact that 36.5% of the flow leaks out of the first set of weirs, the linear velocity, v, of the fluid being pumped through the electroporation zone (Equation 2.6) is thus decreased by the same amount. However, an additional flow due to the EOF generated by the presence of platinum electrodes on the reservoirs had to be taken into consideration to evaluate T_{por}. This velocity can be expressed by

$$v_{eof} = \mu_{eof} \times E \tag{2.9}$$

where μ_{eof} is the mobility due to EOF. The value for μ_{eof} is 4-6 x 10^{-4} $cm^2V^{-1}s^{-1}$. The average value was used for our calculations. The total linear velocity v_t within the liquid is therefore the sum of velocities from pressure driven flow and EOF, i.e.,

$$v_t = v + v_{eof} \tag{2.10}$$

Therefore the pulse time is:

$$T_{por} = \frac{l_e}{v_t} \tag{2.11}$$

In order to obtain the plot in Figure 2.3 we first calculated the electric field from the applied voltage. For the first data point the voltage was 250 V. The voltage drop across the poration zone is 7.04% of the total voltage. Therefore the total voltage drop across a 150 μm poration zone (from Table 2.1) is 7.04% of 250 V or 17.5 V. According to Equation 2.5 the corresponding electric field strength is 1.17 kV/cm. In the first set of weirs 36.5% of the flow is lost. At a volumetric pump rate of 1 μL/min, the linear velocity of the solution inside the poration zone having a width and depth of 50 μm and 20 μm respectively (from Table 2.1) is, according to Equation 2.6

$$63.5\% \times \frac{1\mu L}{\min} \times \frac{\min}{60s} \times \frac{cm^3}{1000\mu L} \div \left(50\mu m \times \frac{cm}{10000\mu m} \times 20\mu m \times \frac{cm}{10000\mu m} \right) \text{ or } 1.058 \text{ cm/s}$$

$v_{eof} = 5 \times 10^{-4} cm^2 V^{-1} s^{-1} \times 1.17 kV cm^{-1} = 0.585$ cm/s according to Equation 2.9. According to Equation 2.10, the total linear velocity v_t during the "on" portion of a cycle is therefore (1.058 + 0.585) cm/s. Therefore, the residence time or pulse time in case of cells is given by

$$T_{por} = 150\mu m \times \frac{cm}{10000\mu m} \div \left(1.643 \frac{cm}{s \times 1000 ms \times s^{-1}} \right) = 9.12 ms$$ according to Equation 2.11.

To determine transfection efficiencies for Figure 2.5 we calculated the amount of plasmid delivered by the pump during the "on" portion of the duty cycle. Then we determined the number of transfectants per microgram of plasmid from the number of colony forming units in Table 2.2. For example, the first data point in Figure 2.5 shows 60 CFU were obtained from plating 100 μL of cells exposed to GFP(uv) on a single plate. The cells collected at reservoir B (Figure 2.1(a)) were diluted to a final volume of 300 μL

(see section 2.2.3). Considering the dilution factors, the total number of transformants for this run was 3 x 60 CFU or 180 CFU. At a pump rate of 1 μL/min, the total amount of 6.17 ng/μL concentration plasmid consumed during the on portion of 75 one second pulses at a 50% duty cycle is $75 \times 0.5s \times \frac{1\min}{60s} \times \frac{1\mu L}{1\min} \times \frac{6.17ng}{1\mu L} \times \frac{1\mu g}{1000ng}$ or 3.86 x 10^{-3} μg of plasmid. The efficiency is the number of transfectants divided by the amount of plasmid consumed or $\frac{180CFU}{3.86 \times 10^{-3}\mu g}$ or 4.67 x 10^4 transfectants per μg plasmid.

2.3.2 Operational Parameters and Chip Performance

The primary figure of merit for transfection is the efficiency, expressed as the number of colony forming units (CFU) obtained per μg of DNA plasmid. The key factors in conventional electroporation are the type of cell to be transfected, the concentration of cells and DNA, the electric field, and the pulse time of the field. E. coli require a higher field strength than other cells do, yet they are commonly used in recombinant DNA work due to their availability, ease of handling and existing protocols.

Depending on the orientation of the electrodes, the direction of the EOF could be the same or the opposite of that of the pressure driven flow. This effect creates a pulse time either larger or smaller than that expected for pressure driven flow alone. Electric fields were applied to the electroporation zone in pulses of 0.5 s in both the same and opposite directions of pressure driven flow. In order to capture more cells within the electroporation zone, obtain a higher fluorescence signal and clear the electroporation zone from blockage due to the accumulation of cell debris on the sides of the channel, Ca^{2+} experiments were performed in an opposing EOF mode. Transfection experiments,

on the other hand, were performed with EOF in the same direction to reduce uncertainty in T_{por}. Pulsing the electric field allowed a cooling period to reduce Joule heating effects.

Cell and DNA concentrations were not varied substantially in this study, rather optimal values used in conventional systems were adjusted to suit the specific demands of the chips. We used a higher DNA concentration and a lower cell concentration. Cell concentrations higher than 5×10^8 tend to plug the weirs. This concentration is considered to be very low for transfection experiments. We therefore used the highest concentration of DNA commercially available and made no further dilutions. For conventional systems 1 μL of 1 ng/μL concentration plasmid is mixed with 40 μL of 1×10^{10} cells/mL or higher concentration of cells. We used 2 μL of 500 ng/μL concentration plasmid for 160 μL of 1.7×10^8 cells/mL of cells corresponding to a plasmid concentration of 6.17 ng/μL in the cell solution. In the flow through design we utilized the residence time in the electroporation zone, which was controlled by the flow rate and could be adjusted with the pump rate and the applied voltage. This residence time is equivalent to the pulse time in conventional systems. However, the field strength and the residence time could not be controlled independently, as the EOF contribution to overall flow rates varied with the applied field. The EOF could be made to oppose the flow rate, or to operate in the same direction by changing the sign of the applied field, leading to drastically different effects on residence time.

Figure 2.3 shows the variation in field strength and residence time in the electroporation zone as a function of applied voltage. For this plot, the field caused EOF in the same direction as the flow of the syringe pump, and the residence times were determined as discussed in section 2.3.1.1 The fields obtained were low for

electroporation of E.coli, which give highest efficiencies at values of 13 to 17 kV/cm [7], but are in the ranges frequently used with larger cells such as yeast and mammalian hosts. The maximum field was limited by the large potential drops across the weirs, so that higher fields tended to cause boiling and arcing at the weirs. However, the residence times we have estimated for this design are consistent with those frequently used for most cells, which range from about 3-50 ms.

By using high voltage relays a square wave voltage pulse was readily generated, allowing the use of a 50% duty cycle with a period of 1 s for the electroporation zone. The duty cycle allowed regular clearing and cooling of the electroporation zone in absence of a field. The use of a pulsed duty cycle was necessary to avoid plugging of the channels with cells.

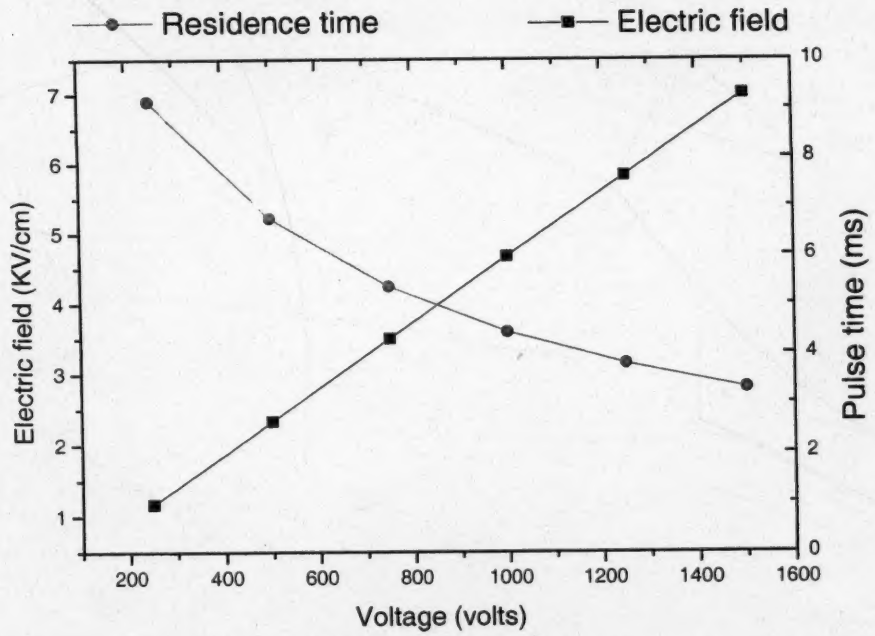

Figure 2.3 Graph of electric field and residence time as a function of applied voltage. Pump rate maintained at 1μL/min.

2.3.3 Electroporation and Ca Ion Uptake

The efficacy of the design for electroporation was first studied by evaluating the uptake of Ca^{2+} from the buffer solution as a function of applied field. In order to increase the residence time significantly, the field was applied to give an EOF in opposition to the pressure driven flow. E. coli cells were readily observed accumulating in the electroporation zone during the "on" portion of the duty cycle. Fluorescence detection was performed inside the electroporation zone. Figure 2.4 shows the increase in fluorescence intensity observed as a function of applied voltage. Visual observation confirmed that significant fluorescence was observed only during the "on" portion of the duty cycle, indicating that electroporation and Ca^{2+} uptake was achieved as a result of the applied field.

2.3.4 Electroporation and Transfection

The uptake of Ca demonstrated the cells could be electroporated, but did not provide any information about their subsequent health or recovery from poration. The uptake and subsequent expression of DNA plasmids with specific protein sequences provides a definitive evaluation of cell status after poration. Two different plasmids were tested within the device, pbluescript skII+ and PGFPuv. The former expresses beta-galactosidase and can be used with indicators to produce blue colonies when the gene is expressed. The latter expresses a UV excitable form of green fluorescent protein fused to beta-galactosidase, which may be directly determined by UV fluorescence on an agar plate.

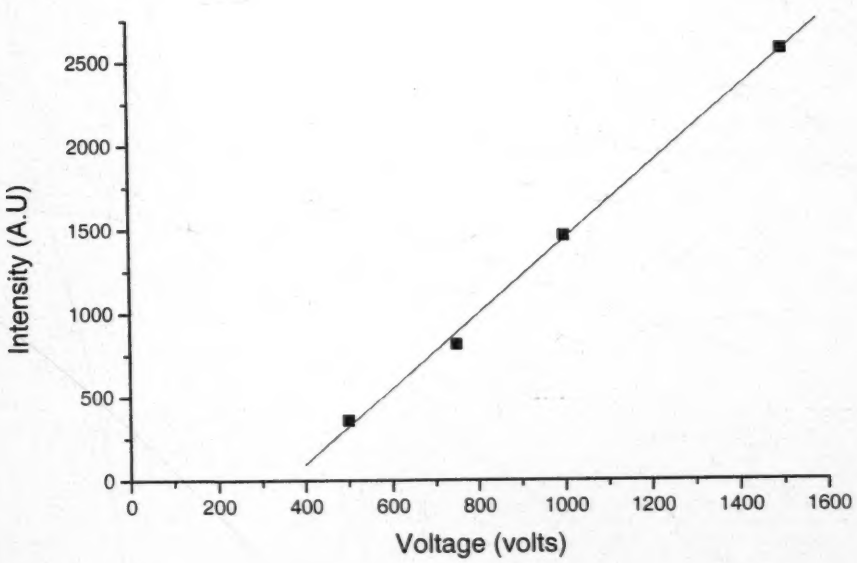

Figure 2.4 Graph of fluorescence as a function of applied voltage. Pump rate was maintained at 1μL/min

E.coli cells were introduced into the chip in an electroporation buffer with 6.17 ng/μL plasmid present and subjected to a range of applied fields. In order to provide a reasonable estimate of residence times, the EOF and pressure driven flow were in the same direction. Approximately 100 μL of solution was collected at the outlet reservoir of

the main channel, transferred to 200 μL LB media and then plated onto ampicillin-loaded agar plates in 100 μL aliquots. Figure 2.6 shows images of typical colonies formed on the plates. Figure 2.5 shows how the transfection efficiencies increased with the applied field for the two different plasmids. Table 2.2 shows the corresponding number of colonies per plate and pulse times obtained for each run. Values for efficiencies, field strengths and pulse times were calculated according to section 2.3.1.1

The transfection efficiencies obtained are lower than those obtained in conventional systems, in part due to the lower electric fields that could be applied and in part due to the lower concentration of cells, differences in processing the cells after electroporation and efficiency loss due to leakage. Nevertheless, the data clearly demonstrates the ability of the star intersection design to induce electroporation and transfection of E. coli cells with genetic material. In addition, the transfection results show that it is possible to recapture small quantities of cells from a microchip and use them again within the laboratory.

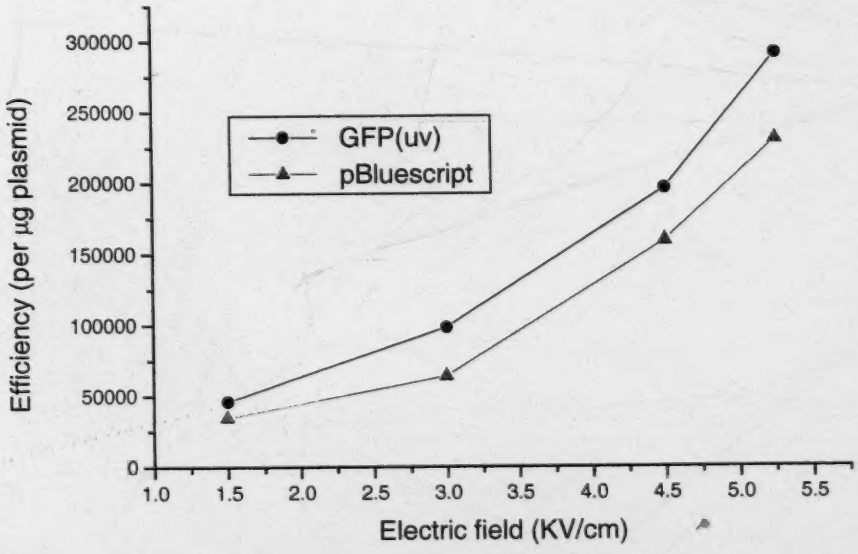

Figure 2.5 Graph of transfection efficiency as a function of electric field. Pumprate was maintained at 1μL/min

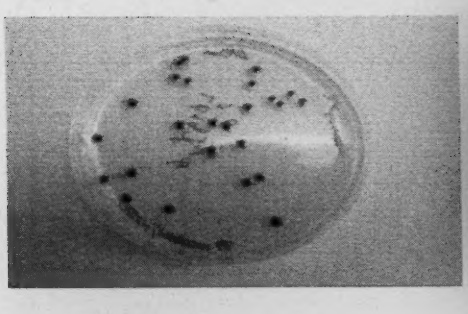

Colonies containing pbluescript

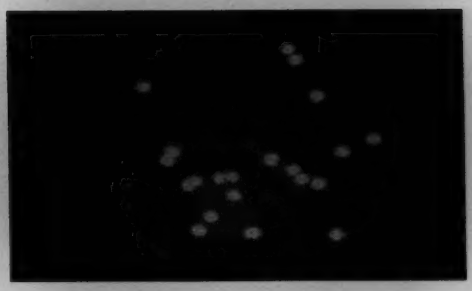

Colonies containing GFP

Figure 2.6 Transfected colonies on agar plates.

Table 2.2 CFU and pulse time data for 3 μm weir hydrochip

CFU for GFP(uv)/plate	CFU for pBluescript/plate	Applied Voltage(V)	Electric Field (kV/cm)	Pulse time for each run (ms)
60	45	321	1.5	8.29
128	83	643	3.0	5.86
255	207	964	4.5	4.53
379	300	1125	5.25	4.07

* CFU per run = 3 x CFU per plate (see section 2.3.1.1 for transfection efficiency calculation)

2.4 Conclusions

Transfection efficiencies for this study were on the order of 1 x 10^5, which is 3 to 4 orders of magnitude less than that obtained by commercial instruments for E. coli cells. The Hydrochip had several limitations to its design. Maximum electric fields of 5.5 kV/cm were obtained with this device, which is not sufficient for high efficiency E.coli transfection. Due to its intricate star like structure a substantial number of cells leaked into and clogged the weirs. The fact that we were unable to use a cell concentration

higher than 1.7 x 10^8 cells/mL also contributed to lower efficiency. In spite of these drawbacks, our results demonstrate that it is feasible to perform bacterial cell electroporation on a microfluidic chip. The work provided a basis for re-designing such a chip, as is described in Chapter 3.

2.5 References

1. Berglund, D. L.; Starkey, J. R. *J. Immunol. Methods* 1989, 120, 79-87.
2. Abdul-Baki, A. A.; Saunders, J. A.; Matthews, B. F.; Pittarelli, G. W. *Plant Sci.* 1990, 70, 181-190.
3. Alexander, J. E.; Andrews, P. W.; Jones, D.; Roberts, I. S. *Lett. Appl. Microbiol.* 1990, 10, 179-181.
4. Fluri, K.; Fitzpatrick, G.; Chiem, N.; Harrison, D. J. *Anal. Chem.* 1996, 68, 4285-4290.
5. Sweedler, J. V.; Shear J. B.; Fishman, H. A.; Zare, R. N.; Scheller, R. H. *Anal. Chem.* 1991, 63, 496-502.
6. Longwell, P. A. *Mechanics of Fluid Flow*, McGraw Hill, New York, 1966.
7. Dower, W. J.; Miller, J. F.; Ragsdale C. W. *Nucleic Acids Research* 1988, 16(13), 6127-6145.

Chapter 3: Single Channel Electroporator for Higher Transfection Efficiency

3.1 Introduction

The hydro chip was initially fabricated as an electro osmotic pump to maneuver or to lyse cells within a channel. The cross, or star intersection on the hydro chip was designed to lyse cells. The cross design of the hydrochip looked promising for performing electroporation on a chip since this process requires a lower voltage and shorter time than does lysis. The device proved very successful in demonstrating electroporation on microfluidic chips. Our ability to perform the Ca^{2+} up take experiments (Section 2.2.3) was also due to its unique cross like structure, which enabled monitoring fluorescence signal in a reverse EOF mode of operation, prompting cells to accumulate in the cross region. Realizing its potential for integrating biological cell processing steps encouraged us to develop a more efficient method of electroporation on-chip. Our goal was to deliver higher electric field strength than the 5.5 kV/cm possible on the hydrochip. Although most mammalian cells can be electroporated with this field, it is not optimal for most bacterial cell transfection. The low transfection efficiencies with the hydro chip resulted mainly from this cause. Table 3.1(a) and 3.1(b) show desired electroporation parameters for a selected number of both bacterial and mammalian cell lines. Consideration of these values prompted us to design a device capable of generating electric fields from as low as several hundred V/cm to tens of kV/cm. Such a device would cover the range of electric fields required for any type of cell transfection with electroporation.

Table 3.1(a) parametres for transfection of common bacteria cell lines.

Cell line	E. Field (kV/cm)	Transfectant	Pulse time (ms)
Agrobacterium tumefaciens	14.4	pGP213	5.0
Bacillus thuringiensis strains	12.5	pHT3101	25
Bacillus subtilis PB1424	6.25	PB1424	5.4
E.coli MC 1061, LE 392	2.5	pUC12	5.1
E. coli DH5α, DH10	12.25	pUC12	5 - 6
Lactobacillus acidophilus ADH	6.25	pGK12	14
Lactobacillus fermentum 1750	6.25	pGK12	14
Lactococcus lactis subsp. *lactis* LM0230	17	pGB301	5
Mycobacterium aurum	12.5	PAL8 DNA	3.5 - 4.5
Pasteurella haemolytica	12.5	pPH33	25
Salmonella Typhimurium DB9008 *Streptococcus*	17	pSA3	5
Streptococcus cremoris Wg2L	5	PAMB13	5
Streptococcus pyogenes T253C	17	pSA3	5
Fremyella diplosiphon (cyanobacteria)	5.5	PBR322	5
Acetobacter xylinum	9.0	pUC18-824, ABCD,tac,lac,bcs	17.7
Helicobacter pylori	12.5	-	5
Clostridium perfringens	6.5	-	5
Haemophilus Influenzae	12.5	PER194, pJ1-8	7.5-9.3
Rhodopseudomonas virldis	12.5	-	14
Campylobacter jejuni	12.5	PTNS #A, pTNS #B	3.5 - 6.5

Table 3.1 (b) Transfection parameters for common mammalian cell lines.

Mamalian cell line	E. Field (kV/cm)	Transfectant	Pulse time(ms)
EMBRYONIC STEM CELLS (D3 cells)	0.8	Linearized vector DNA	0.5
Rat Pituitary Tumor (GH_3)	0.60	pSV2CAT (supercoiled)	5.1
Human Fibroblasts GM0847	1.0	pLAMO (linearized with EcoR1)	0.2
Human Cervical Carcinoma cells (HeLa)	0.65	pMT-hGH-SV2	7
Human hepatocellular carcinoma Hep G2	0.50 - 0.55	pSV2Aluc	30
Primary Human Fetal Fibroblasts IMR-90	0.60	pMT-hGH-SV2	7
Human Hematopoietic K562	1.14 - 1.86	pRSV-neo	2.3 - 3.4
Jurkat Cells	0.63	pSV2Aluc	30
LBRM cells (mouse T-cell lymphoma)	0.875	general	12 – 16
Primary Human Peripheral Blood Lymphocytes	0.63	CMV - CAT pBL3CMV	45 – 50
Primary Human Peripheral Blood Lymphocytes CCRF-CEM T – Lymphoblastoid cells	0.55	pBL3CMV	50 – 55
J558L mouse myeloma	0.875	pLW4	~ 12
HuT 78 Human T-cell lymphoma	0.75	pSIV LTR/CAT, pSV/tat	~ 4
COS 7 cells	0.75	CDNA clones encoding for a receptor for hGM-CSF-R	8.3 – 10.5
Human Neuroblastoma TP410N	1.0	-	7-8
RED BLOOD CELLS	3.5	Inositol hexaphosphate(IHP)	3.1
SP2 lymphoid Cells	0.5	PSV2gpt with a chimeric heavy chain gene	15
Human Melanoma Cell SKMe125	0.625	-	15
Hepatoma Cells (FT02B)	1.75		13
Fetal Cervical Epithelial Cells	5k	HPV DNA (human papillomavirus)	0.5
Human 293 Cells (Embryonic Kidney Cells)	0.675	-	9.5-10
Breast Carcinoma MCF-7	0.75		10
B-Lymphocyte	1.050	PGL2-control, pCAT-control	13

Besides electric field, there were other design problems with the hydrochip. In the cross region cells could easily clog the weirs, inducing failure, or making the device hard to clean after operation. Among other problems, generation of bubbles at the weirs was a major one. It was extremely difficult to remove a bubble of air from within the weir, yet once formed it had to be removed, due to its adverse affect on the applied poration field. The only way to remove a bubble was to apply a vacuum, which proved extremely troublesome. One of the other major reasons for low efficiency in the hydrochip was due to the use of a low cell concentration. Higher cell concentration solutions could not be pumped through the device due to clogging of the weirs. The plugs formed could not be flushed, even with 1 M NaOH. The long channels in the hydrochip meant more pressure was required to produce flow through the channels. This compelled us to use very robust fittings to interface the chip with the syringe, which leaked if not properly secured. Our study of the hydrochip provided the necessary information to design a more suitable electroporation chip. Two different types of designs were evaluated to produce a suitable chip. These designs are discussed in the next few sections.

3.2 Design Concepts

3.2.1 Embedded Electrode Design

All commercially available electroporation apparatus' consist of a cuvette in which cells are loaded and electroporation is done. The spacing between the electrodes in a standard cuvette is 2 mm. Our design goal is to miniaturize such a device by bringing the electrodes closer together and reducing the total volume of a standard 400 μL cuvette. To perform electroporation with bacteria it is necessary to produce electric fields of up to

18 kV/cm. In order to estimate suitable size ranges for the desired fields a few simple calculations were performed. The key to producing high intensity electric fields is to apply a large voltage across a small distance. However, when the conductor is a liquid high voltages cause electrolysis. It is therefore desirable to fix V or L and optimize the other in order to get the highest field without bubble generation.

A design of an electroporator with embedded electrodes requires electrodes fabricated on the sidewalls or bottom of a channel. The area of the electrodes defines the cross section of the electric field. A cell solution can then be made to flow through the electric field. The time the cells spend in the field is the electroporation pulse time. Table 3.2 shows how narrow the spatial gap between electrodes must be in order to achieve high fields with voltages low enough to hope to avoid electrolysis. It can be seen these gaps are extremely small, given the size of the cells and the problems we saw with plugging when cells passed through a 3 μm gap in a weir (Section 2.3.1.1).

The gap described above could be designed in the three following ways. In the simplest approach two metallized plates could be sandwiched together with a thin spacer and sealed at the edges. Alternatively, electrodes could be embedded in channels. In one approach they would be facing each other across a gap, in another they could be placed side by side along one surface of the channel. For the first two designs, the narrow gap we estimate is needed would mean that rapid clogging would be a problem. For the side by side design, the fringing field lines would mean the fields were highly non uniform, and high fields would exist in only a small fraction of the flow path. Our analysis indicates electrodes arranged across a gap to achieve electroporation are impractical, at least with DC voltages.

Table 3.2 Electric field strengths between two metal plates separated by different gaps.

Gap (μm)	Electric field at different voltages (kV/cm)		
	1 V	3 V	5 V
1	10	30	50
3	3.33	10	16.66
5	2.00	6	10
7	1.42	4.29	7.14

The discussion above shows that generating electric fields on the order of tens of kilovolts per cm would definitely cause hydrolysis of the cell solution, for any reasonable channel width, leading to bubble generation and excessive Joule heating. However, if the current in the system can be alternated at a high enough frequency so as to eliminate bubble formation, this problem may be averted.

To investigate the effects of using an AC power supply in an embedded electrode device we evaluated a similar device published by A. P. Lee et al [1], used instead as a magneto hydrodynamic micropump. It is a device that utilizes the Lorentz force to propel electrolyte solution within a microchannel. When an electric field is applied across a channel in the presence of a magnetic field that is perpendicular to it, the Lorentz force is perpendicular to both the electric and magnetic fields, and will induce flow of ions and solvent along a channel. Those authors used high frequencies to avoid the generation of bubbles due to electrolysis. Table 3.3 reports the frequency versus " bubble threshold" field data they obtained. The observed maximum electric field strengths are an order of magnitude lower than what we require for bacterial cell electroporation at the bubble current threshold, making Lee's device unsuitable for our purpose. However, his

data suggest that, if we reduce the gap in between the electrodes tenfold to about 30 μm, the device would produce electric fields within the lower limits of our goal. In doing so we have added the complication of using an oscillating field. The frequency of the current will play a major role in the efficiency of transfection. Radio frequency (1 MHz) modulated square pulses of 2.5 ms have also been used to electroporate streptomyces cells in 13-14 kV/cm fields [2]. Thus it may be possible to work at high enough frequencies to avoid bubble formation, yet still achieve the fields needed to perform electroporation on-chip. This is a promising concept that could be explored in the future, but obviously there is some uncertainty as to how effective it would be.

Table 3.3 Maximum electric field strength to avoid bubbles for different frequencies applied to electrodes spaced 300 μm apart, at different NaCl concentrations.

Frequency (kHz)	Electric field strength for various conc. NaCl solution (kV/cm)		
	0.01 M NaCl	0.1 M NaCl	1 M NaCl
1	0.222	0.321	0.110
10	0.278	0.555	0.251
100	0.389	0.524	0.311
10000	2.499	0.971	0.428

3.2.2 Single Channel Electroporator

The above considerations show that for dc fields the use of embedded electrodes would be difficult. Returning to a fluid channel design for the field delivery brought us to the concept of the use of a constriction or weir to form the high field region in the chip. The hydrochip gave low fields because so much of the voltage drop occurred at the weirs, which were intended to restrict fluid flow. However, if the weirs are redesigned so the cells flow through them, the high impedance of this region can be used to "concentrate" the voltage drop. In order to make this device practical we needed to use a single flow path, avoiding the need for any other flow restrictor. In order to fabricate a continuous flow system incorporating electroporation, a system had to be designed where cells could enter and exit the system freely, without causing any clogging effects.

Obtaining a high electric field within a single channel requires some specific considerations. We first had to determine a practical working distance from one end of the channel to the other. Considering the space required to fit reservoirs and fittings on a chip we designed a 1 cm long channel. To eliminate the possibility of excessive Joule heating and bubble formation in large regions of the flow path, yet obtain a high enough field for electroporation, we placed a weir in the middle of the channel. Evaluating the channel and weir dimensions we discovered that a single channel porator could provide electric fields higher than 20 kV/cm in the weir at an operating voltage of only 2000 V when using the right dimensions. The average electroporation pulse time, ie. the time a cell spends in the weir, could then be determined by the EOF and pump flow rate of the system. The only drawback to this design arises from the effects of EOF, which make it harder to establish the actual flow rate. However, these effects can be eliminated if EOF

Table 3.4 Pulse times for a single channel electroporator with different weir lengths and voltages.

Weir length(μm)	Voltage (V)	Flow Rate(μL/min)	Pulse Time with EOF (ms)		Pulse Time with no EOF (ms)
			+	-	
200	883	1	2.51	-2.85	42
		10	1.63	-7.31	4.2
		20	1.17	9.87	2.1
		30	0.92	3.01	1.4
450	1259	1	5.64	-6.40	94.5
		10	3.67	-16.73	9.45
		20	2.64	22.28	4.72
		30	2.07	6.64	3.15
950	2009	1	11.91	-13.52	199.5
		10	7.75	-34.66	19.95
		20	5.58	47.00	9.97
		30	4.36	14.00	6.65
1450	2759	1	18.18	-20.64	304.5
		10	11.82	-52.97	30.45
		20	8.51	71.61	15.22
		30	6.66	21.37	10.15
700	1633	1	8.77	-9.97	147
		10	5.71	-25.58	14.7
		20	4.11	34.56	7.35
		30	3.21	10.31	4.9
1200	2384	1	15.04	-17.08	252
		10	9.78	-43.79	25.2
		20	7.05	59.36	12.6
		30	5.51	17.69	8.40
1700	3133	1	21.32	-24.21	357
		10	13.86	-62.12	35.7
		20	9.99	83.97	17.85
		30	7.80	25.05	11.9

* Length of channels = 0.5 cm. Channel width = 600μm, Depth = 150 μm. Weir width = 350 μm, Depth = 10 μm. Electric Field was kept constant at 15.0 kV/cm. + EOF implies that the pump flow and EOF are in the same direction while – EOF implies the opposite. A negative pulse time implies that the EOF is greater than the flow rate in the opposite direction.

can be partially or totally removed. Table 3.4 shows the performance of a single channel electroporator operating at different flow rates and voltages. It is evident from this table that this device is capable of creating electric fields and pulse times well within the range needed for bacteria and mammalian cell transfection, whether EOF is present or not. All seven of the devices in Table 3.4 were evaluated, however, only the first four were adopted for the mask design discussed in Section 3.3.1. Calculations to obtain pulse

times are discussed in Section 3.2.2.1. Having considered the pros and cons of all the designs it was decided that the single channel porator device would best serve our purpose

3.2.2.1 Evaluation of E, T_{por} and Transfection Efficiency

According to Figure 3.2 the single channel electroporator can be considered to be an equivalent of a series of 3 resistors. If the resistance of the channels are R and that of the weir or electroporation zone is R_e then, $R = l\rho/A$ and $R_e = l_e\rho/A_e$ where l and A are the lengths and cross sections of the channels, respectively, and subscript e stands for the electroporation zone. Therefore, if the total voltage applied across the electroporator is V_T, then the fraction of voltage drop across R_e is $R_e/(2R + R_e)$ and the voltage drop V, across R_e is,

$$V = \frac{R_e V_T}{(2R + R_e)} \tag{3.1}$$

The electric field strength E across R_e is $E = V/l_e$. Having evaluating the electric field strength, the nominal electroporation time or pulse time for the cells, T_{por}, can be determined as $T_{por} = l_e/v$, where v is the total linear velocity within the channel (see Section 2.3.1.1). In order to obtain pulse times in Table 3.4 for a 200 μm weir device operating at 883 V (15 kV/cm) we determined the voltage drop across the weir from Equation 3.1.

$$V = \frac{\dfrac{200\mu m \times \rho}{350\mu m \times 10\mu m}}{2 \times \dfrac{5000\mu m \times \rho}{600\mu m \times 150\mu m} + \dfrac{200\mu m \times \rho}{350\mu m \times 10\mu m}} \times 883V = 300V$$

Electric field strength, $E = \dfrac{V}{l_e} = \dfrac{300V}{200\mu m} \times \dfrac{10000\mu m}{1cm} = 15000$ V/cm or 15.0 kV/cm

According to Equations 2.6, 2.9, 2.10 and 2.11 from Chapter 2,

$$v = \frac{\phi}{A} = \frac{\frac{1\mu L}{1\min} \times \frac{1\min}{60s} \times \frac{1cc}{1000\mu L}}{(350\times10^{-4}cm \times 10\times10^{-4}} = 0.476 \text{ cm/s}, \quad (2.6)$$

$$v_{eof} = \mu_{eof} \times E = 5\times10^{-4} cm^2V^{-1}s^{-1} \times 15.0kVcm^{-1} = 7.497 \text{ cm/s} \quad (2.9)$$

$$v_t = v + v_{eof} = 7.973 \text{ cm/s} \quad (2.10)$$

$$T_{por} = \frac{l_e}{v_t} = \frac{200\mu m \times \frac{1cm}{10000\mu m}}{7.973cms^{-1}} \times \frac{1000ms}{1s} = 2.51ms \quad (2.11)$$

The value of μ_{eof} of 5 x 10^{-4} cm2$V^{-1}S^{-1}$ is a typical, representative value for glass chips. The nominal linear velocity is the sum of the linear velocity generated by the pump and that generated by EOF. These two flow rates can be in the same or in opposite directions. We refer to this velocity as the nominal value due to the complicating effects that EOF plays in a closed system like ours. In our design, the pump flow and EOF are in the same direction. The pump delivers a constant volume of liquid. When the field is on and inducing EOF in the same direction of flow as the pump, a negative pressure builds up in the channel at the pump head. Because there are no leaks in the system, this negative pressure would have to be counter balanced by fluid flowing into the channel from the open waste reservoir, creating a circulating back flow. In some regions, near the channel walls the flow rate could be close to the nominal value, while in the center of the flow path the negative pressure would create a flow in the opposite direction, with a slightly reduced rate. The net flow that the system will deliver to the outlet reservoir will be that of the pump alone. To prove the existence of this re-circulating flow we performed an experiment discussed in Section 3.4.4. Hence, for the sake of simplicity, we

term the linear velocity with the field on as the nominal linear velocity. We don't know how many times a given cell may be re-circulated, so the nominal velocity gives a lower limit on T_{por}.

Figure 3.1 shows the relationship for minimum pulse time vs nominal flow rate taking the direction and magnitude of EOF into account. These values were estimated for a 150 μm deep device with a 10 μm deep, 450 μm long weir. The operating voltage was 1200 V, which yields an electric field of 12.8 kV/cm. Due to the fact that estimates of pulse time are prone to more error when the EOF opposes the pump flow rate, our experiments were performed with pump and EOF flow in the same direction.

Table 3.5 Values for pressure drops across channels for different dimension porator devices.

Weir length (μm)	Δp_{weir} (psi)	$\Delta p_{channel}$ (psi)	$\Delta p_{Total}=\Delta p_{weir}+2\Delta p_{channel}$ (psi)	Q (μL/min)	F_c	F_w
200	0.34	3.40×10^{-3}	0.35	20	0.10432	0.00935
450	0.76		0.77			
950	1.60		1.61			
1450	2.45		2.45			
700	1.18		1.19			
1200	2.03		2.03			
1700	2.86		2.88			

* Pressures are calculated using Equation 3.1 with $\eta = 1.x\ 10^{-3}$ pascal second at 20 deg C [3]. F_c and F_w are the geometric form factors for the channel and the weir, respectively.

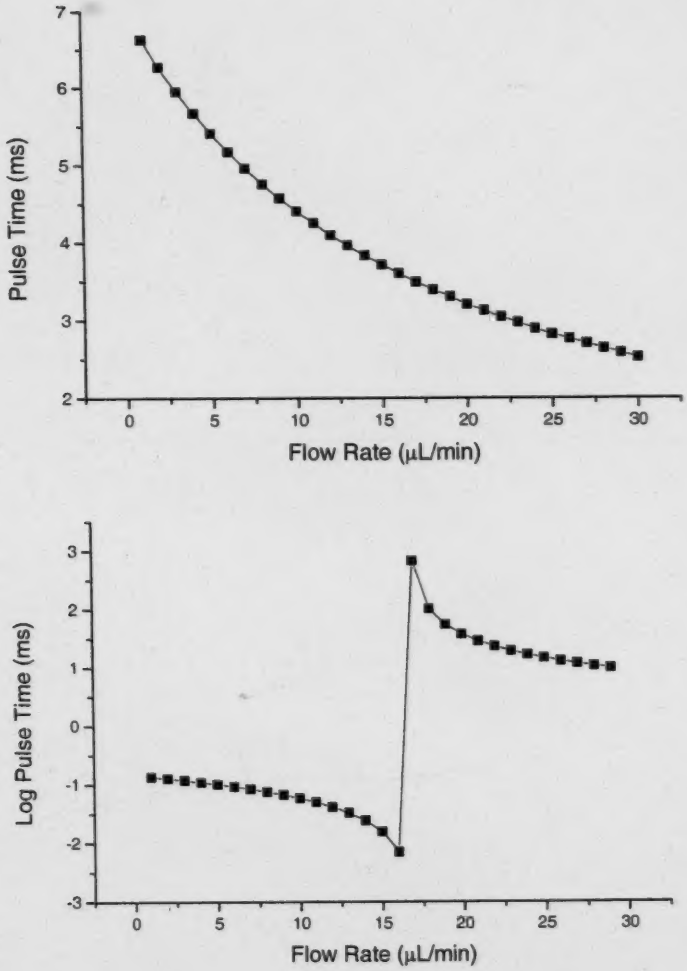

Figure 3.1 Graphs of minimum pulse time vs nominal flow rate for (1) pump flow and EOF in the same direction (upper curve) and (2) opposite direction (lower curve). Negative pulse times are used to indicate that the EOF is greater in magnitude than the pump flow.

3.2.2.2 Determination of Resistance to Pressure Driven Flow

A major issue as to whether the electroporator could function in a pressure driven system had to be resolved. This was done by calculating the pressure drop required to generate the desired volumetric flow rates and comparing them to the pressure that the pump could generate and the fittings could withstand. The pressure drops for the channels and weirs were estimated using the solution of the Navier Stokes equation for a rectangular channel. The pressure drop across the channel is,

$$\Delta p = \frac{4Q\eta l}{w^2 d^2 F} \tag{3.1}$$

where Q is the volumetric flow rate inside the channel, w, d and l are the width, depth and length of the channel respectively and η is the viscosity of the fluid. F [4,5] is a geometrical form factor that can be calculated as follows.

$$F = \frac{w}{3d} - \frac{64w^2}{\pi^2 d^2} \sum_{n=0}^{\infty} \frac{\tanh\left\{\frac{(2n+1)}{2w}\pi d\right\}}{(2n+1)^5}$$

It has been calculated that the pressure drops across the channels for our device are well within the pressures that can be generated with our pump, which is 1000 psi for a 1 mL syringe [6]. Table 3.5 shows these values for different dimension devices.

3.3 Experimental

3.3.1 Chip Design

The Photo masks for the single channel porator chip were fabricated on a 5" x 5" x 0.09" soda lime glass substrate by Adtek (photomask, Montreal, QC, Canada). 32 devices were laid out on a single wafer. A two mask set (Figure 3.2) with various dimensions was used to fabricate the devices. Two slightly different design types were made. The first type consisted of a weir in between two large channels that tapered at the weir.

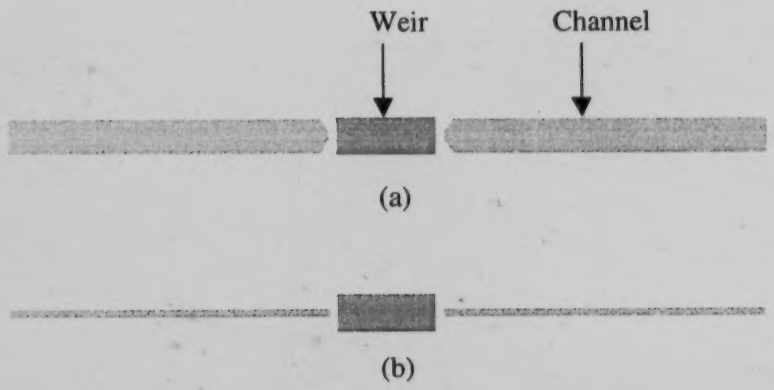

Figure 3.2 (a) Single channel porator with tapered channels and (b) without tapered Channels. Light gray specifies first mask and dark gray specifies second mask.

The feature sizes in the mask for the deep channels were 0.5 cm long and 300 μm wide. The weir's feature sizes were 180, 430, 930, and 1430 μm long and 330 μm wide. The other design consisted of the same dimensions except the large channels were not tapered. In total each weir size was repeated in a set of seven tapered and one non-tapered devices on the same wafer. The spacing between the channels and weirs were laid out according to conditions for a 150 μm etch on a 0211 4" x 4" glass substrate.

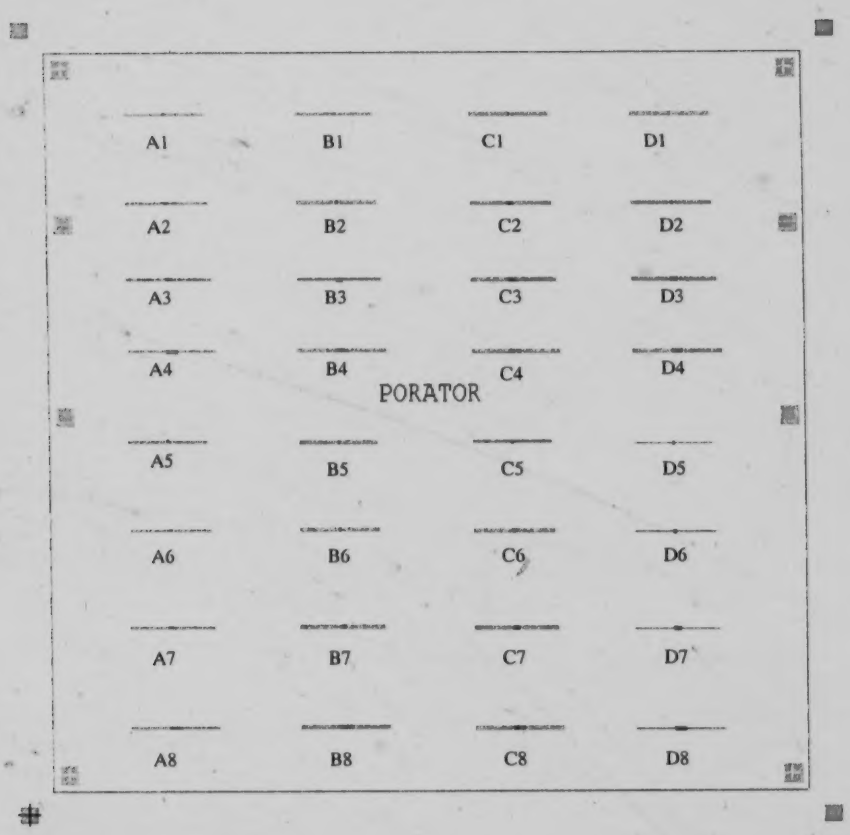

Figuge 3.3 layout of poratorchip showing an array of 32 devices on a single 4" x 4" wafer.

Table 3.6 Weir lengths for porator chip.

Device	Weir Length (μm)	Device	Weir Length (μm)	Device	Weir Length (μm)	Device	Weir Length (μm)
A1	76.8	B1	N/A	C1	N/A	D1	N/A
A2	328.3	B2	326.4	C2	316.8	D2	314.9
A3	825.6	B3	325.6	C3	825.6	D3	325.6
A4	1324.8	B4	1324.8	C4	1305.6	D4	1315.2
A5	76.8	B5	76.8	C5	96	D5	85.5
A6	307.2	B6	326.4	C6	349.4	D6	345
A7	806.4	B7	816	C7	825.6	D7	864
A8	1324.8	B8	1305.6	C8	1305.6	D8	1365

* Channel length, width and depth are 5000 μm, 605± 2 μm and 115 μm respectively.
* Weir length depth and width are 12.5 μm and 355± 1 μm respectively.

Figure 3.3 shows a lay-out of the porator chip. Table 3.6 gives the dimensions of the channels after performing a 150 μm glass etch. These dimensions were measured using an Alpha step profilometer.

3.3.2 Chip Fabrication: Problems, Solutions, and Real Time Chip Performance

The porator chip was fabricated the same way as described in section 2.2.1, however, certain problems arose due to the very deep channel etching done with HF. To avoid problems with photoresist deposition, exposure time was increased from 4 to 10 s. New alignment icons, described in Section 3.4.1 were developed, as a requirement of the deep etch procedure. Other fabrication steps were the same as described in Chapter 2.

3.3.2.1 Constant Channel Depth Upon Deep Etch

Having submerged the substrates in HF for a 150 μm etch time, it was found that a channel depth of more than 115μm was not attainable. Metal mask failure after extended etching periods lead to greater etching along the wafer surface than down into the material. The processed 115 μm deep chips were used successfully.

3.3.3 Transfection Parameters to be Optimized

In order to successfully transfect bacterial cell lines there are a number of factors that must be taken into account before electroporation is performed. Variability in results from strain to strain occur within the same species. For our experiments Dh5α strain of E.Coli bacteria best served our purpose, due to the fact that it is a well known strain, it is easy to handle and cultivate, much has been done with this strain in the literature. It is a harmless strain, making it less hazardous to deal with.

An important aspect to electroporation is to produce electro-competent cells. This was done by culturing cells and freezing them in their mid log phase(discussed in Section

2.2.2) and then washing several times to get rid of any salts that might create sparking within the channels. Growth media can also influence the efficiency of transfection. DNA size also plays a role in transfection efficiency. Smaller super coiled DNA can be transfected more easily than larger linear DNA. Our studies involved the transfection of pGFP(uv) which is a suitable plasmid for E.Coli transfection. Another advantage for pGFP(uv) is that transfected colonies fluoresce brightly under uv light making them very easy to identify and count.

Plating techniques are crucial in obtaining consistent colony counts on a plate. While plating it is necessary to ensure that the spreader used for plating is properly disinfected with ethyl alcohol and is not too hot for plating the cell solution on to the agar plate.

3.3.4 Cell Growth, Preparation and Chip Operation

Cells were cultivated and prepared for transfection experiments according to Section 2.2.2. The cell concentration in the glycerol stock was estimated to be 2.5×10^9 cells/mL. In order to perform transfection experiments with plasmids, a stored vial of cells was thawed on ice and washed 3 times using 1mL dd H_2O. The cells were resuspended in 1 mL dd H_2O. 160 µL of this solution was transferred to an Eppendorf tube in which 4 µL of 1 ng/µL GFP(uv) plasmid was added and mixed with the flick of a finger. This cell solution was used for many of the transfection experiments, except where indicated.

A reservoir was glued on to one end of the porator channel. The chip was flushed with degassed ddH_2O for 30 min in order to have the chip clean and free of any NaOH left from previous washing. The chip was then ready for use. The cell solution was

loaded in a 100 µL gas tight syringe (SGE syringe, gastight 100 µL RN, 25ga, Pt#2, Austin, TX, USA). The syringe was mounted on a syringe pump (PHD 2000, Harvard Apparatus, Holliston, MA, U.S.A) and was connected to peak tubing (0.063 " OD, 0.005 " ID, SPE Ltd., Concord, ON, Canada) using a union fitting (Valco instrumentation company, ON, Canada).

A special kind of device had to be made in order to apply a voltage across the channel and connect the syringe peak tubing to the chip. This device was made by cutting a pipette tip on both ends. One end was cut to fit snugly on the hole of the cover plate above the channel. The other end was cut out to a size slightly larger than the outer diameter of the peak tubing. The peak tubing was inserted into the larger end of the cut pipette tip and a pt electrode was inserted next to it. The rim of the larger end was then sealed with epoxy glue making it leak proof. The narrow end was snugly fit to the chip and the protruding Pt electrode was connected to the power supply. Figure 3.4 shows a schematic drawing of this device.

Once the syringe containing the cell solution was connected to the chip, the reservoir was emptied and filled with 100 µL dd H_2O for receiving the cells. The reservoir end of the channel was set to ground by inserting a Pt electrode connected to the power supply. Pulses at a certain voltage with a 50% duty cycle were applied, using the relays and computer program used in Section 2.2.1, to the cells flowing through the channel at different flow rates. Having completed the pulses, cells were collected from the reservoir with a pipette, in a volume of about 100 µL, diluted to 300 µL. Then, 100 µL of this solution was plated on ampicillin agar plates containing IPTG (see Section 2.2.3). Transfection efficiency was determined by counting the number of colonies on

the plate under UV light and calculating the number of transfectants per μg of plasmid. Further dilution of cells in 100 μL of the reservoir volume was not accounted for in the calculation because it causes a negligible effect on the final result.

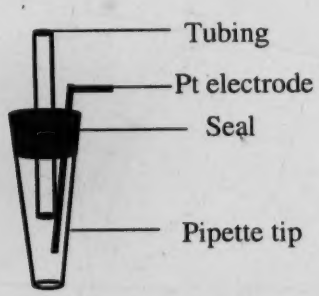

Figure 3.4 Device to connect peak tubing to microchip

To determine transfection efficiencies in Figure 3.6 we first determined the total amount of plasmid consumed during 75 pulses. Evaluation of transfection efficiency is determined in a manner similar to that in Section 2.3.1.1, except that the total time the voltage was cycled was used, instead of just the "on" portion of the cycle.

3.4 Results and Discussion

3.4.1 Designing Special Icons for a Double Mask Deep Etch Technique

Structures having different depths usually require more than a single master mask. Unique icon features are needed that enable alignment, in order to place a master mask above a previously processed substrate to add the additional features. HF etching on glass surfaces is an isotropic process, hence while designing a master mask the effects of under etching the metal layer defining the channel must be taken into account. Etching a 150 μm deep channel results in under etching 150 μm back under the metal mask on the substrate surface. Figure 3.5a shows an icon used for a double mask process for a

shallow etch (< 20 μm) design. We were concerned that a 150 μm under cut would cause the suspended metal film to fail. Our previous alignment marks were designed to align with an intact metal film. We concluded we would need marks that aligned with the etched substrate instead, given that the metal film was likely to crumble. Figure 3.5b shows the modified icon used for our device. It is evident from the dimensions and design of the icon that it is possible to retain alignment accuracy by stripping off the metal layers of the substrate after the first mask photolithography and etching steps. Having completed a 150 μm etch, the metal layers on the substrate failed. By stripping off the metal layers on our new designed icon we were able to align the second mask with the substrate.

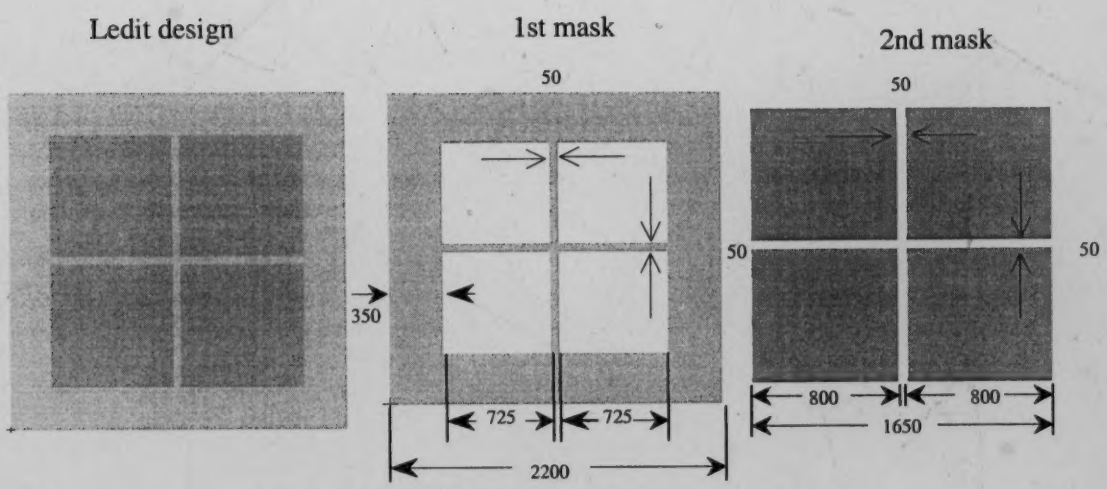

Figure 3.5 (a) Icon for a shallow etch double mask process. Units in microns.

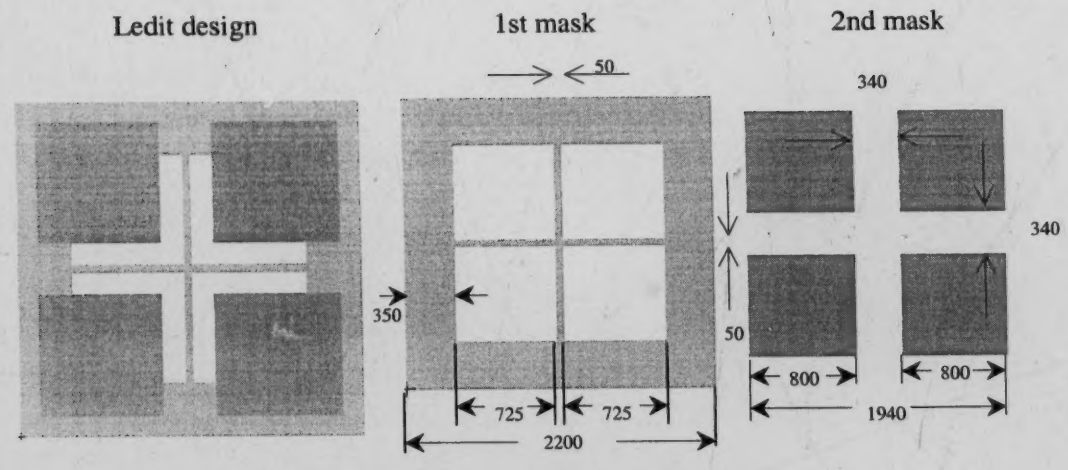

Figure 3.5 (b) Icon for a regular double mask process. Units in microns.

3.4.2 Streak Marks of Photoresist on Substrate

Having completed the first etching with HF the substrates undergo a second round of photolithography. However, if the channel features are very deep, as in our case it, is difficult to create a thin film of photoresist on the substrate. We observed a streaking effect originating at points of the substrate having deep features, causing non-uniform photoresist spreading. This caused an incomplete development of photoresist, rendering the chip useless. In order to overcome this problem, exposure times on the mask were increased from 4 sec to 10 sec, which enabled a complete development of photoresist resulting in functional chips.

3.4.3 DNA and Cell Concentration

Two other important parameters that control transfection efficiency are DNA concentration within the cell solution and the cell concentration. If the DNA concentration is too high then the transfection efficiency reduces due to saturation of DNA. It is therefore essential to work with a high DNA concentration and gradually

decrease it until optimum conditions are obtained. The maximum DNA concentration used in our previous experiments with the hydro chip was 500 ng/μL, which corresponds to a concentration of 6.17 ng/μL within the cell solution. Regarding cell concentration, it is essential that it be very high and preferentially above 1 x 10^{10} cells/μL. Due to the complex structure of the hydrochip it was too difficult to use such a high concentration of cells. Lower concentrations led to a low transfection efficiency. In contrast, in the porator chip cell concentrations as high as 2.5 x 10^{10} could be pumped through the device without creating any clogging within the channel.

Among the electrical parameters, the voltage and the electroporation time or pulse time, T_{por}, had to be optimized before performing electroporation. A voltage drop across the porator channel had to be selected in order to generate the right magnitude of electric field within the weir. This was done using the calculations in Sec 3.2.2.1. In commercially available electroporation instruments most experiments with E.Coli are performed at 13-17 kV/cm electric field within a pulse time of 2 to 5 ms [6]. In order to achieve such performance our experiments were conducted from 900 V to 1300 V to provide an electric field of 9-13 kV/cm within the weir. Higher electric fields were desirable, but not attainable, due to excess current and bubble generation at the weir causing an error in the instrumentation used to generate the electric pulses.

The minimum electroporation pulse time, T_{por}, was calculated from the volumetric flow rate from the pump and the EOF (discussed in section 2.3.1.1). In order to generate 2 to 5 ms pulses for the cells, the volumetric flow rates were varied from 1 to 20 μL/min . T_{por} is heavily dependent on EOF. In order to decrease or preferably eliminate this dependency it is necessary to reduce or eliminate EOF by using coated chips. However,

our experiments were performed with the effects of EOF. This study is basically an extension of the hydrochip work. Optimizing the electroporation conditions using previous data from the hydrochip provided useful performance with the single channel porator chip.

3.4.4 Determination of Re-Circulating Flow in Channel

In order to determine whether there exists re-circulating flow in the channel during the presence of electric field and pressure flow simultaneously we performed an experiment in which Protein A beads (polysciences, Inc, PA, USA) were used to inspect the channel flow during pulsing, using a CCD camera. A 0.133 mg/mL concentration slurry of the beads was prepared in dd H_2O. The size of the beads were 1-2 μm and they were red in color. The pump was set to deliver dd H_2O at a volumetric flow rate of 1 μL/min to the chip. Having turned the pump on, the cell receiving reservoir was filled with the bead slurry. At 1200 V, 25 pulses of 50% duty cycle and 1 s period were applied to the solution. During the pulsing the weir was visually monitored using a CCD camera. It was observed that the protein A beads had traveled upstream from the reservoir to the weir. Our result demonstrates that re-circulating flow due to EOF within a closed channel is a factor within these devices. This unfortunately complicates evaluation of T_{por}.

3.4.5 Dependence of Transfection Efficiency on Electric Field and Pulse Time

Having optimized electroporation conditions, experiments were performed to evaluate the effect of electric field strength and pulse time on transfection efficiency. Experiments were performed at voltages ranging from 900 V to 1300 V, using device A2 (Table 3.6), to determine the optimum voltage for maximum electroporation. These

voltages correspond to an electric field of 9.3 to 13.5 kV/cm. At these settings the electroporation time, T_{por} was calculated to be 4.6 to 6.5 ms. The pump was run at 1 μL/min. 75 one second pulses with a 50% duty cycle were applied across the channel. The cell concentration was 2.5 x 10^9 cells/mL. 4 μL of 1 ng/μL concentration plasmid was added to 160 μL of cells. This corresponds to a plasmid concentration of 24.4 ng/mL cell solution. Having completed 75 cycles the cells were collected from the reservoir and diluted to 300 μL with LB media. Upon 30 minutes of incubation in a shaker at 250 rpm and 37 deg C, 100 μL of the cells were plated on an ampicillin agar plate containing IPTG and incubated at 37 deg C for 15 hours. The plates were then inspected under a uv lamp for GFP colonies. The colonies were easily counted and the transfection efficiency was calculated for each run according to Section 3.4.

Figure 3.6 shows the dependence of transfection efficiency on the electric field intensity. Maximum electroporation occurs around 12.5 kV/cm at 5 ms pulsetime, which is in agreement with existing electroporation techniques for E.Coli transfection. Table 3.7 shows all other parameters for each run. Similar experiments were performed to determine the effect of minimum pulse time on efficiency. Cells were pumped through the electroporator at different nominal flow rates, corresponding to different pulse times. Figure 3.7 shows the efficiency dependence on pulse time. Table 3.8 shows the corresponding nominal flow rates for these pulse times and all other parameters.

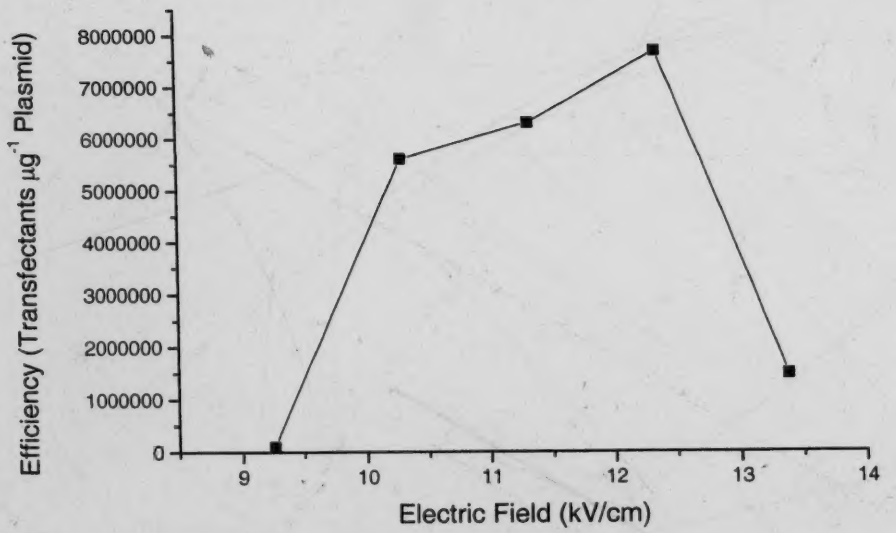

Figure 3.6 Graph of electric field versus efficiency. Pump rate was maintained at 1 µL/min. Data for device A2 (see Table 3.6).

Table 3.7 Parameters for efficiency vs electric field studies.

Voltage (V)	E. Field (kV/cm)	CFU	Efficiency (transfectants/µg DNA)	Flow Due to EOF (µl/min)	Nominal Flow Rate (µL/min)	Nominal Velocity in Weir (cm/s)	Minimum Pulse Time (ms)
900	9.26	1	9.84×10^4	12.33	13.33	5.00	6.55
1000	10.29	57	5.61×10^6	13.70	14.70	5.52	5.94
1100	11.32	64	6.30×10^6	15.07	16.07	6.03	5.43
1200	12.35	78	7.68×10^6	16.44	17.44	6.55	5.01
1300	13.38	15	1.48×10^6	17.81	18.81	7.06	4.64

* Data for device A2 (see Table 3.6)

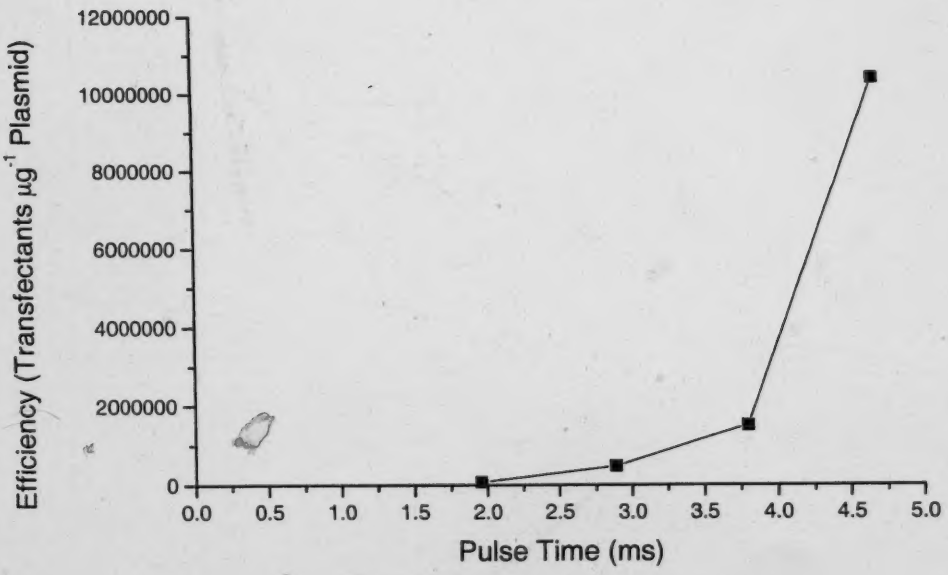

Figure 3.7 graph of efficiency vs pulse time. Operating at 1200 V. Data for device A2 (see Table 3.6)

Table 3.8 Parameters for efficiency vs flow rate studies.

Pump rate(µL/min)	Nominal flow rate (µL/min)	Nominal Velocity in Weir (cm/s)	CFU	Efficiency (Transfectants μg^{-1} Plasmid)	Minimum Pulse Time (ms)
0.9	18.71	7.02	96	1.04×10^7	4.67
5.2	23.01	8.64	80	1.51×10^6	3.80
12.4	30.21	11.34	59	4.68×10^5	2.89
26.8	44.61	16.75	19	6.98×10^4	1.96

* Data for device A2 (see Table 3.6)

These experiments were performed at 1200 V, which corresponds to a field strength of 12.4 kV/cm using device A2 (Table 3.6). Having completed a single run the porator channel was flushed with 0.5 M NaOH for 1 min, then with dd H_2O before another run could be done. Our results indicate that transfection efficiency increases linearly with pulse time for our set of conditions. Pulse times longer than 5 ms were not

accessible in device A2 due to the fact that pulse times are limited by the presence of EOF. We performed experiments using devices A2 and B2 (Table 3.6) only. Other devices were not suitable for the experiments because they did not provide the range of pulse times required for the pump rates we used.

3.4.6 Effect of Cell and DNA Concentration on Transfection Efficiency

To determine the optimum plasmid concentration, different amounts of plasmid were mixed to give a 160 μL cell solution. The cell concentration was kept at 2.5 x 10^9 cells/mL. Figure 3.8 shows the dependence of transfection efficiency on plasmid concentration.

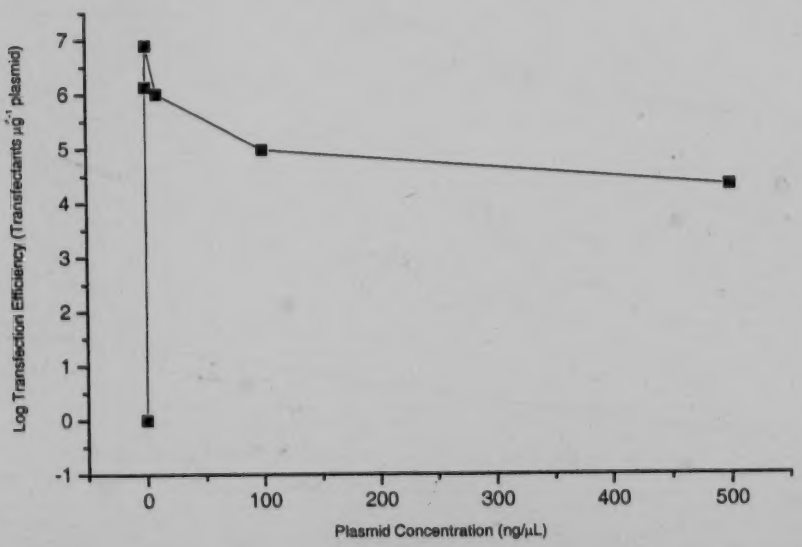

Figure 3.8 Graph of Efficiency vs plasmid concentration. Operating at 1200 V. Pump rate was 1 μL/min Data for B2 device (see Table 3.6). Plasmid concentration corresponds to that before mixing to the cells.

A starting plasmid concentration of higher than 500 ng/μL was not tested because this was the highest concentration obtained from the manufacturer. Table 3.9 shows corresponding CFU s for the different plasmid concentrations at which the experiment

was performed. These experiments were performed at 1200 V, corresponding to 12.4 kV/cm electric field. The pump rate was fixed to 1 μL/min, giving rise to a nominal pump rate of 17.36 μL/min due to EOF. A total of 75 pulses with a 50% duty cycle and 1 s period were applied. The results show that the transfection efficiency increases as the plasmid concentration increases, then decreases, implying an over saturation of DNA in the solution. This is in agreement with transfection protocol for commercially available insruments. Maximum transfection efficiencies using commercial instruments are obtained when a plasmid concentration of 1 to 10 ng/μL is used and the cell concentration is higher than 2.5×10^{10} cells/mL. [7]

Table 3.9 Parameters for Plasmid concentration studies.

Plasmid conc (ng/μL)	CFU	Efficiency(Ttransfectants μg^{-1})
0.1	0	0
0.5	7	1.38×10^6
1	81	7.97×10^6
10	103	1.02×10^6
100	97	9.54×10^6
500	107	2.11×10^4

* Data for device B2 (see Table 3.6)
* Plasmid concentration corresponds to that before mixing to the cells.
* 4 μL of plasmid was mixed with 160 μL of cells.

To study the change in transfection efficiency due to cell concentration we used cell concentrations as high as 1×10^{10}cells/mL. As before, 4 μL of 1 ng/μL concentration plasmid was mixed with 160 μL of cell solution. The voltage was kept at 1200 volts, corresponding to an electric field strength of 12.4 kV/cm. A total of 75 pulses with a 50% duty cycle and 1 s period were applied to different cell concentration solutions. The initial cell concentration was 2.5×10^9 cell/mL and higher concentrations were obtained

by centrifuging and partially removing an appropriate amount of supernatant. The pump flow rate was kept at 1 μL/min, resulting in a 4.96 ms minimum pulse time. Figure 3.9 shows the effect of cell concentration on transfection efficiency and Table 3.10 gives the CFUs for different cell concentration solutions.

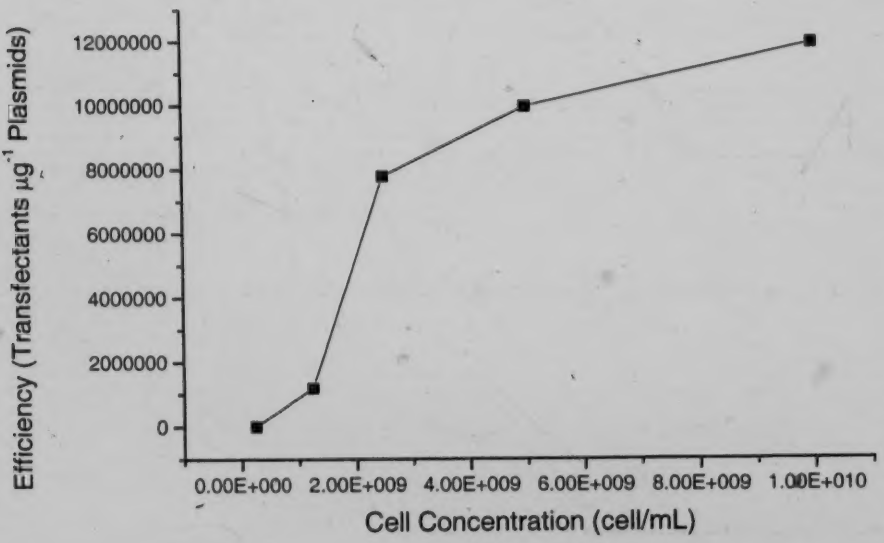

Figure 3.9 Graph of Efficiency vs cell concentration. Operating at 1200 V. Pump rate 1mL/min. Data for B2 Device (see Table 3.6).

Table 3.10 Parameters for cell concentration studies.

Cell conc. (cells/mL)	CFU	Efficiency
2.5×10^8	0	0
1.25×10^9	12	1.18×10^6
2.5×10^9	79	7.77×10^6
5.0×10^9	101	9.94×10^6
1×10^{10}	121	1.19×10^7

* Data for device B2 (see Table 3.6)

We could not perform experiments with higher than 1 x 10^{10} cell/mL because of clogging, followed by bubble formation in the weir. Our results demonstrated that transfection efficiency increases with cell concentration, which is in agreement with current literature. However, the highest efficiency obtained in these experiments, i.e., 1.19 x 10^7 transfectants μg^{-1} plasmid, is still 1 to 2 orders of magnitude below that obtained with commercial instruments. This value is 40 times better than the highest transfection efficiency obtained in Chapter 2, i.e., 2.91 x 10^5.

3.4.7 Chip Sensitive Parameters

Besides the parameters discussed in the above section there are a number of other parameters that need to be addressed that are not significant in common procedures, but may play a significant role for on-chip electroporation. These factors are discussed in the next few sections.

3.4.7.1 Adding Salts to Media During Electroporation

The process of electroporation involves perforation at many sites on the cell surface. This is a harmful process to the cells, causing both permanent and temporary damage, and in many cases destruction of the cell. Having undergone the poration process, a transient process takes place involving an exchange of intra and extra cellular matter through the pores by diffusion. In commercially available devices, electroporation is generally carried out in an electrolyte free media, in order to prevent any sparking which might lead to total cell death. However, the lack of electrolytes within the media causes a cellular imbalance of electrolytes, leading to rapid diffusion out of the cell. In order to reduce this process extra cellular electrolytes may be added to the media. The electrodes in our glass microchip are further separated than a commercially available

instrument. This enables efficient heat dissipation and less sparking even at higher voltages.

In order to increase transfection efficiencies we attempted to add salts to the electroporation media. To investigate this possibility different concentrations of NaCl solutions were prepared. Initially a 1 mM solution was filled in the channel. It was observed that the current was too high above 1100 V, leading to errors in the computer control system, presumably due to arcing. Attempts to fill the channel with higher salt concentration solutions were therefore abandoned.

3.4.7.2 Addition of Broth to Cell Receiving Reservoir and Duty cycle

Inside the electroporation media, cells are in a hostile environment due to the lack of nutrients within their vicinity. Therefore a crucial step towards successful electroporation and transfection is to transfer cell solution to incubating media as soon as the electroporation step is over. This step should be completed within one minute. Delaying the process can lead to decreased transfection efficiencies of 10 to a 100 times. On-chip electroporation allows us to integrate this step within the chip by filling the cell receiving reservoir with broth before applying an electric field to the cells.

The duty cycle for the pulses of high voltages applied across the electroporator can be defined as the ratio of the time on, to the sum of the time on and time off in each consecutive pulse. Our initial experiments with Ca^{2+} (Section 2.3.3) required duty cycles of 50% with a period of 1 sec (0.5 s on + 0.5 s off). The need for a duty cycle came from the observation that continuous voltages applied to cell suspensions in narrow channels and weirs caused clogging or aggregation of the cells. This problem caused a restriction to flow. If the applied voltage is pulsed, this cell accumulation can be avoided to a

substantial extent. Pulses of less than 0.6 seconds with a 50% duty cycle proved to be ineffective for our purpose, due to an error in the computer control system. Arcing due to making and breaking the relay contact was the source of this limitation. Most of our experiments were conducted with 1 s pulses of 50% duty cycle.

Upon visual inspection it was realized that accumulation of cell debris at the weir could be reduced by applying fewer pulses and by increasing the pump flow rate. In an attempt to increase the transfection efficiency we performed an electroporation experiment in which the cell receiving reservoir was filled with 100 μL broth instead of dd H_2O. The flow rate of the pump was increased from 1 μL/min to 10 μL/min. 25 pulses with a 50% duty cycle and 1 s period were applied instead of 75 pulses from previous experiments. This experiment was performed at 1200 V corresponding to an electric field of 12.4 kV/cm. The cell concentration was 2.5×10^9. In order to calculate the efficiency we further increased the dilution of cells after the experiment from 300 μL to 3mL, a 10 fold increase in the dilution factor from previous experiments. Having plated 100 μL of this solution we counted 25 colonies that corresponded to a transfection efficiency of 7.38×10^6 transfectants μg^{-1} plasmid.

3.5 Conclusions

This study was an extension of chapter 2. Modifications in the device design have enabled us to achieve efficiencies about 2 orders of magnitude higher than that obtained for the Hydro device. Due to EOF effects pulse times were uncertain and had to be resolved using average pulse times. Nevertheless this device proved very successful in performing on-chip electroporation with Ecoli. Our results suggest that the single channel device would be a good choice to perform mammalian cell transfection.

3.6 References

1. Lemoff, A. V.; Lee, A. P. *Sensors and Actuators B* 2000, 63, 178-185.
2. Tyurin, M.; Starodubtseva, L.; Kudryavtseva, H.; Voeykova, T.; Livshits, V. *Biotechnology Techniques* 1995, 9(10), 737-740.
3. Longwell, P. A. *Mechanics of Fluid Flow*, McGraw Hill, New York, 1966.
4. Perry, J. H. *Chemical Engineers Handbook*, McGraw Hill, New York, 1950, p-3485.
5. PHD 2000 Syringe Pump Series Users' Manual.
6. Dower, W. J.; Miller, J. F. *Nucleic Acids Res.* 1988, 16(13), 6127-6145.
7. Electro Cell Manipulator 600 Electroporation Protocol for E. coli DH5α, DH1, 1992.

Chapter 4: Conclusions and Future Developments

4.1 Summary

The aim of this thesis was to perform electroporation on a microfluidic chip. We have successfully demonstrated that electroporatiuon can be performed in a continuous flow system with cells that are difficult to transfect, i.e., bacteria cells. This has paved the way for future on-chip electroporation of a whole variety of cell lines.

In Chapter 2, we described how electroporation could be performed on-chip. Many of the parameters essential for E.coli transfection could not be optimized due to device design restrictions. Nevertheless, we succeeded in our goal of transfecting cells. The transfection efficiencies we obtained were much lower than those of commercial instruments. Efficiencies as high as 1×10^{10} transfectants per μg plasmid have been reported in the literature [1]. Values of 1×10^{8} to 1×10^{9} transfectants per μg plasmid are typical using commercial instruments. Our efficiency of 2.91×10^{5} was 4 to 5 orders of magnitude below this value. A substantial portion of Chapter 2 deals with the foundation work to evaluate the effect of important parameters such as electric field, residence time and flow distribution within the chip.

Chapter 3 deals with the challenges of designing and fabricating a new device capable of enhanced performance in terms of transfection efficiency. Besides the fabrication challenges associated with etching deep channels in 0211 glass substrates, effort was made on the design of a device suitable for electroporation of many cell lines. We concluded that embedded electrodes within a channel operating under DC conditions would not be suitable for our purpose. The fact that a high electric field can be produced in the weir, from Chapter 2, helped us realize that weir constriction could be used to

create an electroporation zone. The single channel device enabled us to flow cells through the weir with no clogging, even at cell concentrations as high as 2.5×10^{10} cells/mL. Optimal conditions for Electric field, pulse time, DNA and cell concentration were also evaluated. In terms of performance, this design could produce efficiencies on the order of 1×10^{7} transfectants per μg plasmid, which is only 1 to 2 orders of magnitude lower than that of commercial instruments and certainly within the lower limits of E.coli transfection in general.

4.2 Future Work

4.2.1 Elimination of EOF in channels

Our attempts to determine residence times in Chapter 2 and Chapter 3 have been complicated by EOF. In the hydrochip design we had to take into account additional flow created by EOF to determine residence times. The same was the case for the single channel electroporator except, we had to consider the effect on pulse times in the presence of re-circulating flow in the weir. Residence times calculated for our devices represent a lower limit due to re-circulation. It is therefore desirable to eliminate EOF or at least reduce it substantially in order to quantitatively understand the device performance. This can be accomplished either by coating the channels in the chip [2] or by fabricating chips from material that do not generate EOF. For example, plastic chips have reduced EOF. A device with no EOF would enable us to determine pulse times accurately. It would also enable us to produce long residence times in the presence of high electric field; a limitation of the previous designs.

4.2.2 Electroporation under Reduced Temperatures

Standard protocols for E.coli electroporation require electrocompetent cells to be chilled before electroporation, in order to reduce Joule heating effects. This was not done for our experiments. Performing our experiments under reduced temperature conditions may well have a positive impact upon transfection efficiencies, however, further investigation would be needed.

4.2.3 Mammalian Cell Transfection

Most mammalian cells undergo electroporation with an electric field of several hundred V/cm and 10-50 ms pulse times. The single channel electroporator would be ideal for working with such cells. EOF contribution to additional volumetric flow would drastically be reduced, making residence times more accurate, although with EOF present some re-circulation would still occur. Moreover, excessive current and Joule heating would be reduced low enough to utilize ionic buffers during poration.

4.2.4 Integration to Other On-Chip Processes

A potential application of on-chip cell transfection could perhaps be the coupling of this step to other on-chip biological steps. For example, integrating the single channel electroporator to an on-chip diluter followed by on-chip cell culture stage, with integrated lysing, DNA purification and finally polymerization chain reaction (PCR) incorporated to construct cDNA libraries would definitely be of great value in the field of automation. Examples of on-chip integration have been cited in the literature quite often, however, little includes cell transfection as an intermittent step.

4.2.5 Electroporation using Alternating Current (AC) Electric Fields

Although it is conventional to use DC pulses for electroporation, some studies have been performed to investigate the nature of electroporation using AC pulses. The common problem using DC pulses is that too many cells could be damaged in the process. In AC electroporation, a train of pulses is applied to the cell solution. Studies have been done using DC-shifted sinusoidal waves with frequencies as high as 1 MHz [3,4,5]. Embedded electrodes within a channel operating under 100 V could perhaps be used to perform electroporation in an AC electric field.

4.3 References

1. Dower, W. J.; Miller, J. F.; Ragsdale C. W. *Nucleic Acids Research* 1988, 16(13), 6127-6145.
2. Bibeau, D. R.; Smith K. B.; Smith, E. M.; Ewing, A. G. *J. Microcol. Sep.* 1999, 11(8), 567-575.
3. Shao, X. W.; Shen, Y. F.; O'Neill, K.; Lee, M. L. *J. Microcol. Sep* 1999, 11(5), 325-329.
4. Barberi, R.; Bonvent, J. J.; Bartolino, R.; Roeraade, J.; Capelli, L.; Righetti, P. G. *J. Chromatogr. B* 1996, 683(1), 3-13.
5. Chang, D. C. *Biophys. J.* 1989, 56, 641-652.
6. Tyurin, M.; Starodubtseva, L.; Kudryavtseva, H.; Voeykova, T.; Livshits, V. *Biotechnology Techniques* 1995, 9(10), 7317-740.